

*Chapter 5***5.8.2 Walls**

The plans for the tenant spaces in WTC 1 showed no interior walls whose sole function was to subdivide the floors. There were a number of partitioned offices and conference areas. Although NIST was not able to obtain layout drawings for the fire floors in WTC 2, the verbal descriptions of those floors indicated similarly open space. The types of interior walls were described in Section 5.3.4.

5.8.3 Flooring

Truss-supported concrete slabs formed the floors in the office areas of the towers. Some tenants had installed slightly raised (6 in.) floors on top of the slab under which communication cables were run. This was especially true on trading floors. There was a wide range of floor coverings in use. Inlaid wood and marble were used in some reception areas. Most commonly, the expanse of the floor was covered with nylon carpet.

5.8.4 Ceilings

There were two different ceiling tile systems originally installed in the towers under Port Authority specification. The framing for each was hung from the bottom of the floor trusses, resulting in an apparent room height of 8.6 ft and an above-ceiling height of about 3.4 ft. The tiles in the tenant spaces were 20 in. square, $\frac{3}{4}$ in. thick, lay-in pieces on an exposed tee bar grid system. The tiles in the core area were 12 in. square, $\frac{3}{4}$ in. thick, mounted in a concealed suspension system. Neither system was specified to be fire-rated, and it was estimated that in a fire they might provide only 10 min to 15 min of thermal protection to the trusses before the ceiling frame distorted and the tiles fell. Chemically, the tiles were similar, and their combustible content, flame spread, and smoke production were all quite low.

5.8.5 Furnishings

The decorating styles of the tower tenants ranged from simple, modular trading floors to customized office spaces. The most common layout of the focus floors was a continuous open space populated by a large array of workstations or cubicles (Figure 1-11). The number of different types of workstations in the two towers was probably large. However, discussions with office furniture distributors and visits to showrooms indicated that, while there was a broad range of prices and appearances, the cubicles were fundamentally similar to that shown in Figure 5-8.

The workstations were typically 8 ft square, bounded on all four sides by privacy panels, with an entrance opening in one side only. Within the area defined by the panels was a



Source: Reproduced with permission of The Port Authority of New York and New Jersey.

Figure 5-8. A WTC workstation.

self-contained workspace: desktop (almost always a wood product, generally with a laminated finish), file storage, bookshelves, carpeting, chair, etc. Presumably there were a variety of amounts and locations of paper, both exposed on the work surfaces and contained within the file cabinets and bookshelves. The cubicles were grouped in clusters or rows, with up to 215 units on a given floor.

NIST estimated the combustible fuel loading on these floors to have been about 4 lb/ft² (20 kg/m²), or about 60 tons per floor. This was somewhat lower than found in prior surveys of office spaces. The small number of interior walls, and thus the minimal amount of combustible interior finish, and the limited bookshelf space account for much of the differences. While paper in the filing cabinets might have been significant in mass, it did not burn readily due to the limited oxygen available within the drawers.

Chapter 5

Table 5-3. Floors of focus.

Building	Floor	Tenant	Damage ^a	Fires ^b	Material Obtained ^c	General Description of Tenant Layout
WTC 1	92	Carr Futures, empty		Y	FP (Carr), V	
	93	Marsh & McLennan (M&M), Fred Alger Mgmt.	Y	Y	FP, F, V	M&M occupied the south side. Filled with workstations. Demising walls for the south façade to the edges of the core. Offices along the east side of the south core wall. Stairwell to the 94 th floor.
	94	Marsh & McLennan	Y	Y	FP, F, V	Generally open space filled with workstations. Offices and conference rooms around most of the perimeter. Stairwell to the 93 rd floor.
	95	Marsh & McLennan	Y	Y	FP, F, V	Generally open space filled with workstations. Offices, conferences and work areas in exterior corners. Large walled data center along north and east sides. Two separate stairwells, one to 94 th floor, the other to the 96 th and 97 th floors.
	96	Marsh & McLennan	Y	Y	FP, F, V	Generally open space filled with workstations. Offices at exterior corners and middle of north and south façades. Some conference rooms on north and south sides of core. Stairwell connection to 95 th and 97 th floors.
	97	Marsh & McLennan	Y	Y	FP, F, V	Generally open space filled with workstations. Offices at exterior corners and in the middle of the north façade. Two separate stairwells: one connected to the 95 th and 96 th floors, the other connected to the 98 th , 99 th , and 100 th floors.
	98	Marsh & McLennan	Y	Y	FP, F, V	Generally open space filled with workstations. Offices at exterior corners and middle of north and south façades. Some conference rooms on north and south sides of core. Stairwell connected to the 97 th , 99 th , and 100 th floors.
	99	Marsh & McLennan	Y	Y	FP, F, V	Open space filled with workstations on the east side and east half of the north side. Offices at exterior corners and along south and west sides. Large walled area on west side of north façade. Stairwell connected to the 97 th , 98 th , and 100 th floors.
	100	Marsh & McLennan		Y	FP, F, V	Considerable number of workstations, but more individual offices than the other floors. Partitioned offices extended the full length of the west wall and also at other locations along walls and at exterior corners. Stairway connected to the 97 th , 98 th , and 99 th floors.
	104	Cantor Fitzgerald		Y	V	Trading floor. Tables with many monitors.

The Design and Construction of the Towers

Building	Floor	Tenant	Damage ^a	Fires ^b	Material Obtained ^c	General Description of Tenant Layout
WTC 2	77	Baseline	Y	Y	FP, V	Generally open space. Offices along east and west core walls. A few offices in each exterior corner of the floor.
	78	Baseline, 1 st Commercial Bank	Y	Y	FP, V	West side open. Northeast quadrant walled. Offices along south side of east core wall. Offices along east side of south façade.
	79	Fuji Bank	Y	Y	V	
	80	Fuji Bank	Y	Y	FP, V	Generally open space filled with workstations. Offices or conference rooms at exterior corners and along south half of west façade. Large vault at southeast corner of core.
	81	Fuji Bank	Y	Y	V	
	82	Fuji Bank	Y	Y	V	
	83	Chuo Mitsui, IQ Financial	Y		V	Chuo Mitsui had half the area. Wide open space. No information regarding IQ Financial.
	84	Eurobrokers	Y		V	Open floor for trading. Tables rather than workstations. Perimeter offices.
	85	Harris Beach	Y		FP, V	Offices around full perimeter. Offices along east, west and south walls of core.

a. Floors on which the exterior photographs indicated direct damage from the aircraft.

b. Floors on which the exterior photographs indicated extensive or sustained fires.

c. Types of descriptive material obtained: FP, floor plan; F, documentation of furnishings; V, verbal description of interior.

Chapter 5

This page intentionally left blank.

Chapter 6

RECONSTRUCTION OF THE COLLAPSES

6.1 APPROACH

The following presents an overview of the methods used to reach the accounts in Part I. The details may be found in the companion reports to this document, which are indexed in Appendix C.

A substantial effort was directed at establishing the baseline performance of the WTC towers, i.e., estimating the expected performance of the towers under normal design loads and conditions. This enabled meeting the third objective of the Investigation, as listed in the Preface to this report. The baseline performance analysis also helped to estimate the ability of the towers to withstand the unexpected events of September 11, 2001. Establishing the baseline performance of the towers began with the compilation and analysis of the procedures and practices used in the design, construction, operation, and maintenance of the structural, fire protection, and egress systems of the WTC towers. The additional components of the performance analysis were:

- The standard fire resistance of the WTC truss-framed floor system,
- The quality and properties of the structural steels used in the towers, and
- The response of the WTC towers to design gravity and wind loads.

The second substantial effort was the simulation of the behavior of each tower on September 11, 2001, providing the basis for meeting the first and second objectives of the Investigation. This entailed four modeling steps:

1. The aircraft impact into the tower, the resulting distribution of jet fuel, and the damage to the structure, partitions, insulation materials, and building contents.
2. The spread of the multi-floor fires.
3. The heating of the structural elements by the fires.
4. The response of the damaged and heated building structure, and the progression of structural component failures leading to the initiation of the collapse of the towers.

For such complex structures and complex thermal and structural processes, each of these steps stretched the state of the technology and tested the limits of software tools and computer hardware. For example, the investigators advanced the state-of-the-art in the measurement of construction material properties and in structural finite element modeling. New modeling capability was developed for the mapping of fire-generated environmental temperatures onto the building structural components.

For the final analyses, four cases were used, each involving all four of the modeling steps. Case A and Case B were for WTC 1, with Case B generally involving more severe impact and fire conditions than

Chapter 6

Case A. For WTC 2, Case D involved more severe impact and fire conditions than Case C. The results of the two cases for each tower provided some understanding of the uncertainties in the predictions.

There were substantial uncertainties in the as-built condition of the towers, the interior layout and furnishings, the aircraft impact, the internal damage to the towers (especially the insulation), the redistribution of the combustibles, and the response of the building structural components to the heat from the fires. To increase confidence in the simulation results, NIST used information from an extensive collection of photographs and videos of the disaster, eyewitness accounts from inside and outside the buildings, and laboratory tests involving large fires and the heating of structural components. Further, NIST applied formal statistical methods to identify those parameters that had the greatest effect on the model output. These key inputs were then varied to determine whether the results were reasonably robust.

The combined knowledge from all the gathered data and analyses led to the development of a probable collapse sequence for each tower,¹³ the identification of factors that contributed to the collapses, and a list of factors that could have improved building performance or otherwise mitigated the loss of life.

6.2 DEVELOPMENT OF THE DISASTER TIMELINE

Time was the unifying factor in combining photographic and video information, survivor accounts, emergency calls from within the towers, and communications among emergency responders. The visual evidence was the most abundant and the most detailed.

The destruction of the WTC towers was the most heavily photographed disaster in history. The terrorist attacks occurred in an area that is the national home base of several news organizations and has several major newspapers. New York City is also a major tourist destination, and visitors often carry cameras to record their visits. Further, the very height that made the towers accessible to the approaching aircraft also made them visible to photographers. As a result there were hundreds of both professional and amateur photographers and videographers present, many equipped with excellent equipment and the knowledge to use it. These people were in the immediate area, as well as at other locations in New York and New Jersey.

There was a surprisingly large amount of photographic material shot early, when only WTC 1 was damaged. By the time WTC 2 was struck, the number of cameras and the diversity of locations had increased. Following the collapse of WTC 2, the amount of visual material decreased markedly as people rushed to escape the area and the huge dust clouds generated by the collapse obscured the site. There is a substantial, but less complete, amount of material covering the period from the tower collapses to the collapse of WTC 7 late the same afternoon.

¹³ The focus of the Investigation was on the sequence of events from the instant of aircraft impact to the initiation of collapse for each tower. For brevity in this report, this sequence is referred to as the "probable collapse sequence," although it does not actually include the structural behavior of the tower after the conditions for collapse initiation were reached and collapse became inevitable.

There were multiple sources of visual material:

- Recordings of newscasts from September 11 and afterward, documentaries, and other coverage provided information and also pointed toward other potential sources of material.
- Web sites of the major photographic clearinghouses.
- Local print media.
- NYPD and FDNY.
- Collections of visual material assembled for charitable or historical purposes.
- Individuals' photographs and videos that began appearing on the World Wide Web as early as September 11, 2001.
- Responses to public appeals for visual material by the Investigation Team.

Investigation staff contacted each of the sources, requested the material, made arrangements for its transfer, and addressed copyright and privacy issues. Emphasis was placed on obtaining material in a form as close as possible to the original in order to maintain as much spatial and timing information as possible: direct digital copies of digital photographs and videos, high resolution digitized copies of film or slide photographs, and direct copies from the original source of analog video.

The assembled collection included:

- 6,977 segments of video footage, totaling in excess of 300 hours. The media videos included both broadcast material and outtakes. Additionally, NIST received videotapes recorded by more than 20 individuals.
- 6,899 photographs from at least 200 photographers. As with the videos, many of the photographs were unpublished.

This vast amount of visual material was organized into a searchable database in which each frame was characterized by a set of attributes: photographer (name and location), time of shot/video, copyright status, content (including building, face(s), key events (plane strike, fireballs, collapse), the presence of FDNY or NYPD people or apparatus, and other details, such as falling debris, people, and building damage).

The development of a timeline for fire growth and structural changes in the WTC buildings required the assignment of times of known accuracy to each video frame and photograph. Images were timed to a single well-defined event. Due to the large number of different views available, the chosen event was the moment the second plane struck WTC 2, established from the time stamps in the September 11 telecasts. Based on four such video recordings, the time of the second plane impact was established as 9:02:59 a.m.

The TV network clocks were quite close to the actual time since they were regularly updated from highly accurate geopositioning satellites or the precise atomic-clock-based timing signals provided by NIST as a public service.

Chapter 6

Absolute times were then assigned to all frames of all videos that showed the second plane strike. By matching photographs and other videos to specific events in these initially assigned videos, the time assignments were extended to visual materials that did not include the primary event. Times were also cross-matched using additional characteristics, such as the appearance and locations of smoke and fire plumes, distinct shadows cast on the buildings by these plumes, the occurrence of well-defined events such as a falling object, and even a clock being recorded in an image. By such a process, it was possible to place photographs and videos extending over the entire day on a single timeline. As the time was assigned to a particular photograph or video, the uncertainty in the assignment was also logged into the database. In all, 3,032 of the catalogued photographs and 2,673 of the video clips in the databases were timed with accuracies of ± 3 s or better.

This process enabled establishing the times of four major events of September 11, listed in Table 6–1. The building collapse times were defined to be the point in time when the entire building was first observed to start to collapse.

Table 6–1. Times for major events on September 11, 2001.

Event	Time
First Aircraft Strike	8:46:30 a.m.
Second Aircraft Strike	9:02:59 a.m.
Collapse of WTC 2	9:58:59 a.m.
Collapse of WTC 1	10:28:22 a.m.

There were additional sources of timed information. Phone calls from people within the building to relatives, friends, and 9-1-1 operators conveyed observations of the structural damage and developing hazards. Communications among the emergency responders and from the building fire command centers contributed further information about the areas where the external photographers had no access.

6.3 LEARNING FROM THE VISUAL IMAGES

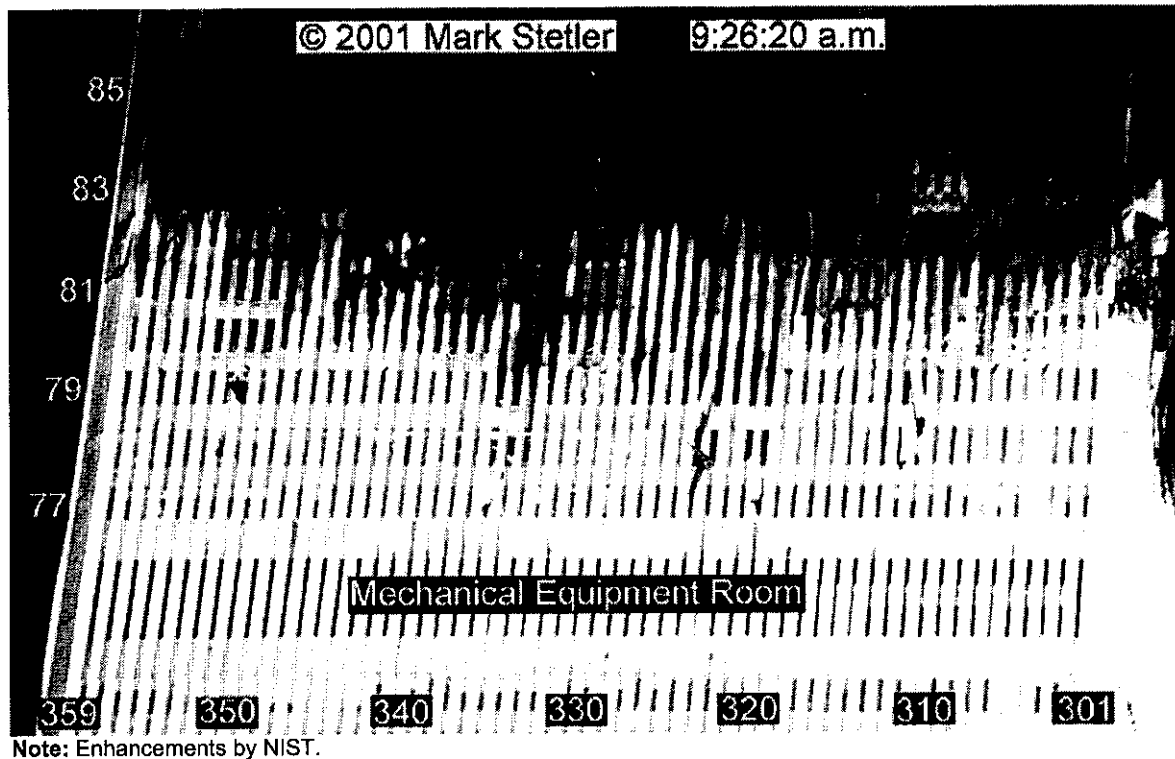
The photographic and video images were rich sources of information on the condition of the buildings following the aircraft impact, the evolution of the fires, and the deterioration of the structure. To enable analysis of this information, a shorthand notation (based on the building design drawings) was used to label the exterior columns and windows of the buildings:

- First, the faces of the towers were numbered in a manner identical to those used in the original plans:

WTC 1:	north: 1	east: 2	south: 3	west: 4
WTC 2:	west: 1	north: 2	east: 3	south: 4
- The 59 columns across each tower face were assigned three-digit numbers. Following the floor number, the first digit was that of the face, and the remaining two digits were assigned consecutively from right to left as viewed from outside the building. Thus, the fourth column from the right on the east face of the 81st floor of WTC 1 was labeled 81-204.

- Each of the 58 windows on each floor and tower face was assigned the number of the column to its right as viewed from the outside of the building and was also identified by its floor. Thus the rightmost window on the east face of the 94th floor of WTC 1 was labeled 94-201.

As an example of information that was extracted, Figure 6-1 shows an enhanced image of the east face of WTC 2. Figure 6-2 expands a section of interest. The amount of detail available is evident. For instance, large piles of debris are present on the north side of the tower on the 80th and 81st floors, and locations where fires are visible or where missing windows are easily identified. Many details of each frame were important in tracking the evolution of the fires and the damage to the buildings.



Note: Enhancements by NIST.

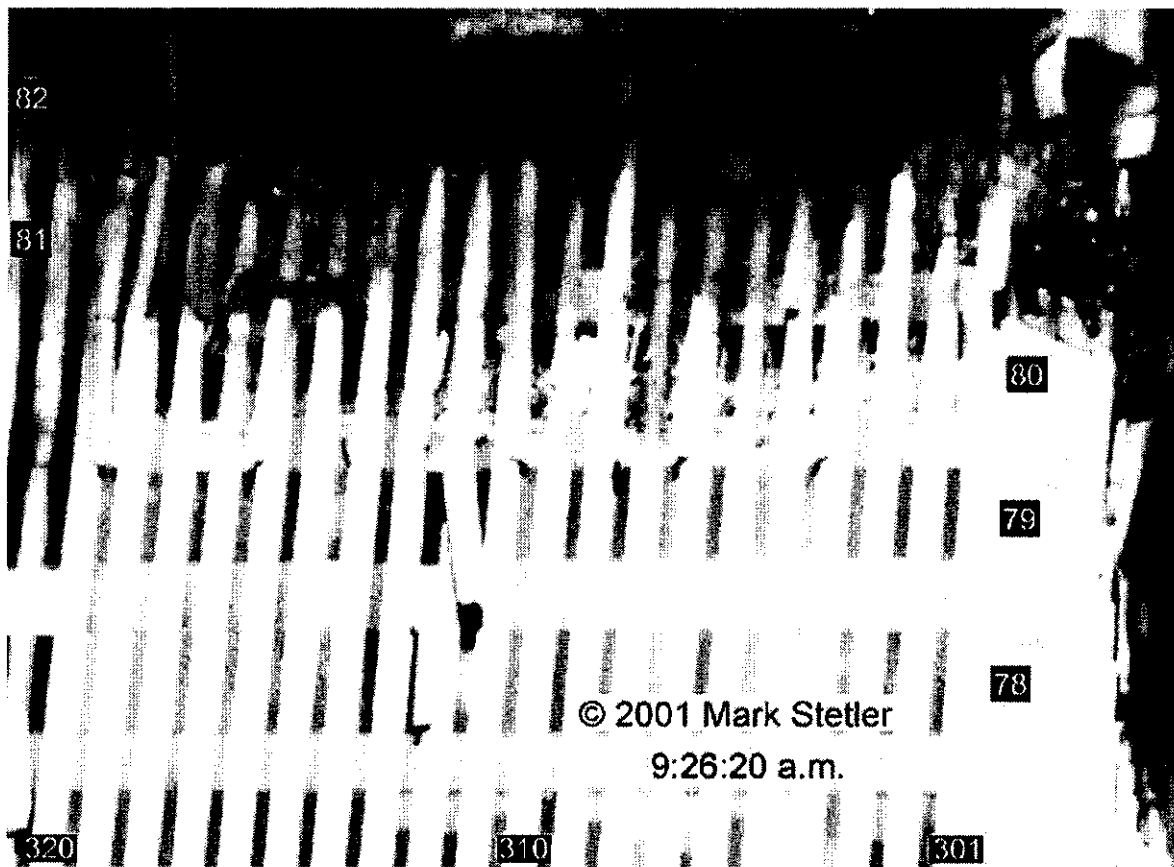
Figure 6-1. 9:26:20 a.m. showing the east face of WTC 2.

In each photograph and each video frame, each window was also coded to indicate whether the window was still in place or not and the extent to which flames and smoke were visible. Color-coded graphics of the four façades of the two towers were then constructed. Examples of these graphics were shown in Chapters 2 and 3.

The results of the visual analysis included:

- The locations of the broken windows, providing information on the source of air to feed the fires within.
- Observations of the spread of fires.
- Documentation of the location of exterior damage from the aircraft impact and subsequent structural changes in the buildings.

Chapter 6



Note: Enhancements by NIST.

Figure 6-2. Close-up of section of Figure 6-1.

- Identification of the presence or absence of significant floor deterioration at the building perimeter.
- Observations of certain actions by building occupants, such as breaking windows.

The near-continuous observations of the externally visible fires provided input to the computer simulations of fire growth and spread. The discrete observations of changes in the displacement of columns and, to a far lesser degree, floors became validation data for the modeling of the approach to structural collapse of the towers. Table 6-2 lists the most important observations.

6.4 LEARNING FROM THE RECOVERED STEEL

6.4.1 Collection of Recovered Steel

NIST had two reasons for obtaining specimens of structural steel from the collapsed towers. The primary objective was characterizing the quality of the steel and determining its properties for use in the structural modeling and analysis of the collapse sequences. The second reason was obtaining information regarding the behavior of the steel in the aircraft impact zone and in areas which had major fires.

Table 6–2. Indications of major structural changes up to collapse initiation.

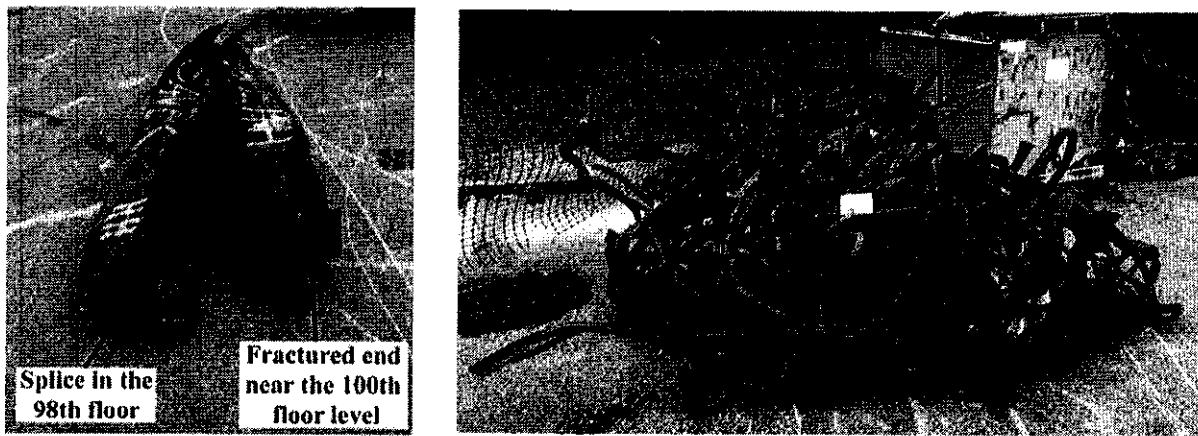
Tower	Time (a.m.)	Observation
WTC 1	10:18	Smoke suddenly expelled on the north face (floors 92, 94, 95 to 98) and west face (92, 94 to 98).
	10:23	Inward bowing of perimeter columns on the east side of the south face from floors 94 to 100; maximum extent: 55 in. \pm 6 in. at floor 97.
	10:28:22	First exterior sign of collapse (downward movement of building exterior). Tilting of the building section above the impact and fire area to due south as the structural collapse initiated. First exterior sign of downward movement of building at floor 98.
WTC 2	9:02:59	Exterior fireball from the east face of floor 82 and from the north face from floors 79 to 82. The deflagration prior to the fireballs may have caused a significant pressure pulse to act on floors above and below.
	9:21	Inward bowing of exterior wall columns on most of the east face from floors 78 to 83; maximum extent: 7 in. to 9 in. at floor 80.
	9:58:59	First exterior sign of collapse (downward movement of building exterior). The northeast corner tilted counterclockwise around the base of floor 82. Column buckling was then seen progressing across the north face and nearly simultaneously on the east face. Tilting of the building section above the impact and fire area to the east and south prior to significant downward movement of the upper building section. The tilt to the south did not increase any further as the upper building section began to fall, but the tilt to the east did increase until dust clouds obscured the view.

Within weeks of the destruction of the WTC, contractors of New York City had begun cutting up and removing the debris from the site. Members of the FEMA-sponsored and ASCE-led Building Performance Assessment Team, members of the Structural Engineers Association of New York, and Professor A. Astaneh-Asl of the University of California, Berkeley, CA, with support from the National Science Foundation, had begun work to identify and collect WTC structural steel from various recycling yards where the steel was taken during the clean-up effort. The Port Authority of New York and New Jersey (Port Authority) also collected structural steel elements for future exhibits and memorials.

Over a period of about 18 months, 236 pieces of steel were shipped to the NIST campus, starting about six months before NIST launched its investigation. These samples ranged in size and complexity from a nearly complete three-column, three-floor perimeter assembly to bolts and small fragments. Figures 6–3 through 6–5 show some of the recovered steel pieces. Seven of the pieces were from WTC 5. The remaining 229 samples represented roughly 0.25 percent to 0.5 percent of the 200,000 tons of structural steel used in the construction of the two towers.

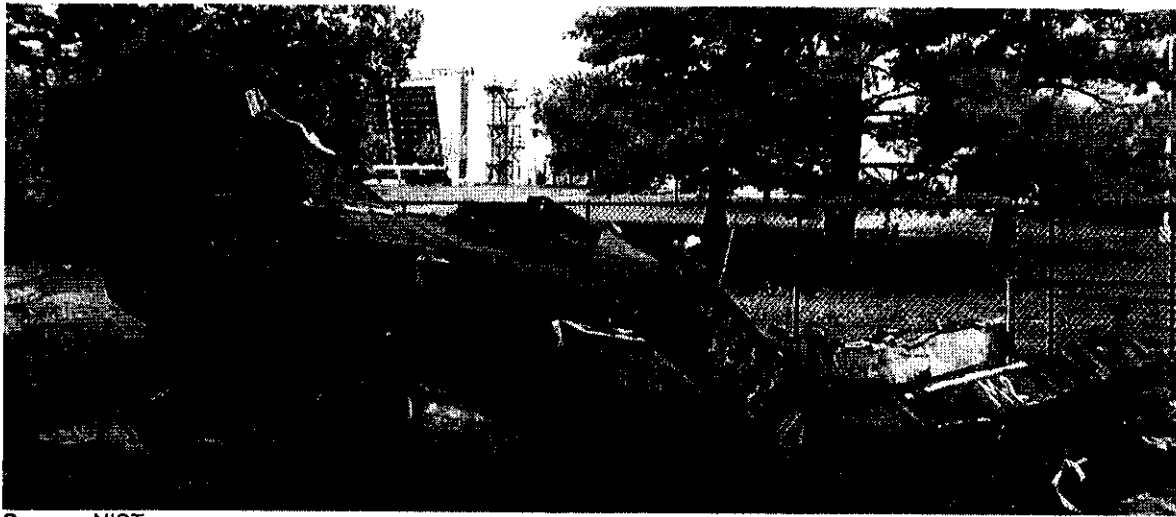
The collection at NIST included samples of all the steel strength levels specified for the construction of the towers. The locations of all structural steel pieces in WTC 1 and WTC 2 were uniquely identified by stampings (recessed letters and numbers) and/or painted stencils. NIST was successful in finding and deciphering these identification markings on many of the perimeter panel sections and core columns, in many cases using metallurgical characterization to complete missing identifiers. In all, 42 exterior panels were positively identified: 26 from WTC 1 and 16 from WTC 2. Twelve core columns were positively identified: eight from WTC 1 and four from WTC 2. Twenty-three pieces were identified as being parts of trusses, although it was not possible to identify their locations within the buildings.

Chapter 6



Source: NIST.

Figure 6-3. Examples of a WTC 1 core column (left) and truss material (right).



Source: NIST.

Figure 6-4. WTC 1 exterior panel hit by the fuselage of the aircraft.

Overlaying the locations of the specimens with photographs of the building exteriors following the aircraft impact (for perimeter columns and spandrels) and the extent-of-damage estimates (Section 6.8) (for core columns) enabled the identification of steel pieces near the impact zones. These included five specimens of exterior panels from WTC 1 and two specimens of core columns from each of the towers.

6.4.2 Mechanical and Physical Properties

NIST determined the properties of many of the recovered pieces for comparison with the original purchase requirements, comparison with the quality of steel from the WTC construction era, and input to the structural models used in the Investigation. Structural steel literature and producers' documents were used to establish a statistical basis for the variability expected in steel properties.

The properties of the steel samples tested were consistent with the specifications called for in the steel contracts. In particular, the yield strengths of all samples of the floor trusses were higher than called for in the original specifications. This was in part because the truss steels were supplied as a higher grade than specified. Overall, approximately 87 percent of all perimeter and core column steel tested exceeded the required minimum yield strengths specified in design documents. Test data for the remaining samples were below specifications, but were within the expected variability and did not affect the safety of the towers on September 11, 2001. Furthermore, lower strength values measured by NIST could be expected due to (a) differences in test procedures from those used in the qualifying mill tests and (b) the damaged state of the samples. The values of other steel properties were similar to typical construction steels of the WTC construction era. The limited tests on bolts indicated that their strengths were greater than the specified minimum, and they were stronger than contemporaneous literature would suggest as typical. The tested welds performed as expected.

NIST measured the stress-strain behavior at room temperature (for modeling baseline performance), high temperature strength (for modeling structural response to fire), and at high strain rates (for modeling the aircraft impact). Based on data from published sources, NIST estimated the thermal properties of the steels (specific heat, thermal conductivity, and coefficient of thermal expansion) and creep behavior for use in the structural modeling of the towers' response to fire.

6.4.3 Damage Analysis

NIST performed extensive analyses of the recovered steel specimens to determine their damage characteristics, failure modes, and (for those near the fire zones) fire-related degradation. In some cases, assessment of enhanced photographic and video images of the towers enabled distinguishing between damage that occurred prior to the collapse and damage that occurred as a result of the collapse. Because the only visual evidence was from the outside of the buildings, this differentiation was only possible for the perimeter panel sections. The observations of fracture and failure behavior, confirmed by an Investigation contractor, were also used to guide the modeling of the towers' performance during impact and subsequent fires and to evaluate the model output.



Source: NIST.

Figure 6-5. WTC 1 exterior panel hit by the nose of the aircraft.

Chapter 6

For two of the five exterior panels from the impact zone of WTC 1, the general shape and appearance of the recovered pieces matched photographs taken just before the building collapse. Thus, NIST was able to attribute the observed damage to the aircraft impact. NIST also made determinations regarding the connections between structural steel elements:

- There was no evidence to indicate that the joining method, weld materials, or welding procedures were inadequate. Fractures of the columns in areas away from a welded joint were the result of stretching and thinning. Perimeter columns hit by the plane tended to fracture along heat-affected zones adjacent to welds.
- The failure mode of spandrel connections varied. At or above the impact zone, bolt hole tear-out was more common. Below the impact zone, it was more common for the spandrels to be ripped from the panels. There was no evidence that fire exposure changed these failure modes.
- The exterior column splices at the mechanical floors, which were welded in addition to being bolted, generally did not fail. The column splices at the other floors generally failed by bolt fracture.
- The perimeter truss connectors (or seats) below the impact zone in WTC 1 were predominantly bent down or torn off completely. Above the impact zone, the seats were as likely to be bent upward as downward. Core seats could not be categorized since their as-built locations could not be determined.
- Failure of core columns was a result of both splice connection failures and fracture of the columns themselves.

Examination of photographs showed that 16 of the exterior panels recovered from WTC 1 were exposed to fire prior to the building collapse. None of the nine recovered panels from within the fire floors of WTC 2 were directly exposed to fire. NIST used two methods to estimate the maximum temperatures that the steel members had reached:

- Observations of paint cracking due to thermal expansion. Of the more than 170 areas examined on 16 perimeter column panels, only three columns had evidence that the steel reached temperatures above 250 °C: east face, floor 98, inner web; east face, floor 92, inner web; and north face, floor 98, floor truss connector. Only two core column specimens had sufficient paint remaining to make such an analysis, and their temperatures did not reach 250 °C. NIST did not generalize these results, since the examined columns represented only 3 percent of the perimeter columns and 1 percent of the core columns from the fire floors.
- Observations of the microstructure of the steel. High temperature excursions, such as due to a fire, can alter the basic structure of the steel and its mechanical properties. Using metallographic analysis, NIST determined that there was no evidence that any of the samples had reached temperatures above 600 °C.

These results were for a very small fraction of the steel in the impact and fire zones. Nonetheless, these analyses indicated some zones within WTC 1 where the computer simulations should not, and did not, predict highly elevated steel temperatures.

6.5 INFORMATION GAINED FROM OTHER WTC FIRES

There had been numerous fires in the towers prior to September 11, 2001. From these, NIST learned what size fire WTC 1 and WTC 2 had withstood and how the tower occupants and the responders functioned in emergencies. While The Port Authority's records of prior fires were lost in the collapses, FDNY provided reports on 342 fires that had occurred between 1970 and 2001.

Most of these fires were small, and occupants extinguished many of them before FDNY arrival. Forty-seven of these fires activated one to three sprinklers and/or required a standpipe hose for suppression. Only two of the fires required the evacuation of hundreds of people. There were no injuries or loss of life in any of these fires, and the interruptions to operations within the towers were local.

A major fire occurred in WTC 1 on February 13, 1975, before the installation of the sprinkler system. A furniture fire started in an executive office in the north end of an 11th floor office suite in the southeast corner of the building. The fire spread south and west along corridors and entered a file room. The fire flashed over, broke seven windows, and spread to adjacent offices north and south. The air conditioning system turned on, pulling air into the return air ducts. Telephone cables in the vertical shafts were ignited, destroying the fire-retarded wood paneling on the closet doors. The fire emerged on the 12th and 13th floors, but there was little nearby that was combustible. The fire also extended vertically from the 9th to the 19th floors within the telephone closet. Eventually the fire was confined to 9,000 ft² of one floor, about one-fourth of the total floor area. The trusses and columns in this area had been sprayed with BLAZE-SHIELD D insulation to a specified ½ in. thickness. Four trusses were slightly distorted, but the structure was not threatened.

Only one major fire incident resulted in a whole-building evacuation. At 12:18 p.m. on February 26, 1993, terrorists exploded a bomb in the second basement underground parking garage in the WTC complex. The blast immediately killed six people and caused an estimated \$300 million in damage. An intense fire followed and, although the flames were confined to the subterranean levels, the smoke spread into four of the seven buildings in the WTC complex. Most of the estimated 150,000 occupants evacuated the buildings, including approximately 40,000 from the affected towers. In all, 1,042 people were injured in the incident, including 15 who received blast-related injuries. The evacuation of the towers took over 4 hours. The incident response involved more than 700 firefighters (approximately 45 percent of FDNY's on-duty personnel at the time).

In addition, there was a fire on the 104th floor of WTC 1 on September 11, 2001, that apparently did not contribute to the eventual collapse, yet was quite severe. At 10:01 a.m., flames were first observed on the west face, and by 10:07 a.m., intense flames were emanating from several windows in the southern third of that face. The fire raged until the building collapsed at 10:28 a.m. Thus, the tower structure was able to withstand a sizable fire for about 20 min, presumably with the ceiling tile system heavily damaged and the truss system exposed to the flames. The 104th floor was well above the aircraft impact zone, so there should have been little damage to the sprayed fire-resistive material, which was the same (Table 5-3) as

Chapter 6

on the floors where the fires led to the onset of the collapse. The photographic evidence showed no signs of column bowing or a floor collapse.

6.6 THE BUILDING STRUCTURAL MODELS

6.6.1 Computer Simulation Software

Structural modeling of each tower was required in order to:

- Establish the capability of the building, as designed, to support the gravity loads and to resist wind forces;
- Simulate the effects of the aircraft impacts; and
- Reconstruct the mechanics of the aircraft impact damage, fire-induced heating, and the progression of local failures that led to the building collapse.

The varied demands made different models necessary, and different software packages were used for each of these three functions. The reason for the choice in each case is presented in the next three sections of the report.

6.6.2 The Reference Models

Under contract to NIST, Leslie E. Robertson Associates (LERA) constructed a global reference model of each tower using the SAP2000, version 8, software. SAP2000 is a software package for performing finite element calculations for the analysis and design of building structures. These global, three-dimensional models encompassed the 110 stories above grade and the six subterranean levels. The models included primary structural components in the towers, resulting in tens of thousands of computational elements. The data for these elements came from the original structural drawing books for the towers. These had been updated through the completion of the buildings and also included most of the subsequent, significant alterations by both tenants and The Port Authority. LERA also developed reference models of a truss-framed floor, typical of those in the tenant spaces of the impact and fire regions of the buildings, and of a beam-framed floor, typical of the mechanical floors.

LERA's work was reviewed by independent experts in light of the firm's earlier involvement in the WTC design. It was that earlier work, in fact, that made LERA the only source that had the detailed knowledge of the design, construction, and intended behavior of the towers over their entire 38-year life span. The accuracy of the four models was checked in two ways:

- The two global models were checked by Skidmore, Owings & Merrill (SOM), also under contract to NIST, and by NIST staff. This entailed ensuring consistency of the models with the design documents, and testing the models, for example, to ensure that the response of the models to gravity and wind loads was as intended and that the calculated stresses and deformations under these loads were reasonable.
- The global model of WTC 1 was used to calculate the natural vibration periods of the tower. These values were then compared to measurements from the tower on eight dates of winds

ranging from 11.5 mph to 41 mph blowing from at least four different directions. As shown in Table 6-3, the N-S and E-W values agreed within 5 percent and the torsion values agreed within 6 percent, both within the combined uncertainty in the measurements and calculations.

- SOM and NIST staff also checked the two floor models for accuracy. These reviews involved comparison with simple hand calculations of estimated deflections and member stresses for a simply supported composite truss and beam under gravity loading. For the composite truss sections, the steel stress results were within 4 percent of those calculated by SAP2000 for the long-span truss and within 3 percent for the short-span truss. Deflections for the beams and trusses matched hand calculations to within 5 percent to 15 percent. These differences were within the combined uncertainty of the methods.

Table 6-3. Measured and calculated natural vibration periods (s) for WTC 1.

	Direction of Motion		
	N-S	E-W	Torsion
Average of Measured Data	11.4	10.6	4.9
Original Predicted Values	11.9	10.4	—
Reference Global Model Predictions	11.4	10.7	5.2

The few discrepancies between the developed models and the original design documents, as well as the areas identified by NIST and SOM as needing modification, were corrected by LERA and approved by NIST. The models then served as references for more detailed models for aircraft impact damage analysis and for thermal-structural response and collapse initiation analysis.

NIST also used these global reference models to establish the baseline performance of the towers under gravity and wind loads. The two key performance measures calculated were the demand-to-capacity ratio (DCR) and the drift.

- Demand is defined as the combined effects of the dead, live, and wind loads imposed on a structural component, e.g., a column. Capacity is the permissible strength for that component. Normal design aims at ensuring that DCR values for all components be 1.0 or lower. A value of DCR greater than 1.0 does not imply failure since designs inherently include a margin of safety.
- Drift is the extent of sway of the building under a lateral wind. Excessive deflection can cause cracking of partitions and cladding, and, in severe cases, building instability that could affect safety.

Using SAP2000, NIST found that, under original WTC design loads, a small fraction of the structural components had DCR values greater than 1.0. (Most DCR values of that small fraction were less than 1.4, with a few as high as 1.6.) For the perimeter columns, DCR values greater than 1.0 were mainly near the corners, on floors near the hat truss, and below the 9th floor. For the core columns, these members were on the 600 line between floors 80 and 106 and at core perimeter columns 901 and 908 for much of their height. (See Figure 1-5 for the column numbers.) One possible explanation to the cause of DCRs in excess of 1.0 may lie in the computer-based structural analysis and software techniques employed for this

Chapter 6

baseline performance study in comparison with the relatively rudimentary computational tools used in the original design nearly 40 years ago.

As part of its wind analysis, NIST calculated the drift at the top of the towers to be about 5 ft in a nearly 100 mph wind—the wind load used in the original design. Common practice was, and is, to design for substantially smaller deflections; but drift was not, and still is not, a design factor prescribed in building codes.

The estimation of wind-induced loads on the towers emerged as a problem. Two sets of wind tunnel tests and analyses were conducted in 2002 by independent laboratories as part of insurance litigation unrelated to the NIST Investigation. The estimated loads differed by as much as 40 percent. NIST analysis found that the two studies used different approaches in their estimations. This difference highlighted limitations in the current state of practice in wind engineering for tall buildings and the need for standards in the field of wind tunnel testing and wind effects estimation.

6.6.3 Building Structural Models for Aircraft Impact Analysis

Ideally, the Investigation would have used the reference global models of the towers as the “targets” for the aircraft. However, this was not possible. The impact simulations required inclusion of both a far higher level of detail of the building components and also the highly nonlinear behavior of the tower and aircraft materials, and the larger model size could not be accommodated by the SAP2000 program. There were also physical phenomena for which algorithms were not available in this software. Another finite element package, LS-DYNA, satisfied these requirements and was used for the impact simulations.

Early in the effort, it became clear to both NIST and to ARA, Inc., the NIST contractor that performed the aircraft impact simulations, that the model had to “fit” on a state-of-the-art computer cluster and to run within weeks rather than months. To minimize the model size while keeping sufficient fidelity in the impact zone to capture the building deformations and damage distributions, various tower components were depicted with different meshes (different levels of refinement). For example, tower components in the path of the impact and debris field were represented with a fine mesh (higher resolution) to capture the local impact damage and failure, while components outside the impact zone were depicted more coarsely, simply to capture their structural stiffness and inertial properties. The model of WTC 1 included floors 92 through 100; the model of WTC 2 extended from floor 77 through floor 85. The combined tower and aircraft model of more than two million elements, at time steps of just under a microsecond, took approximately two weeks of computer time on a 12-noded computer cluster to capture the needed details of the fraction of a second it took for the aircraft and its fragments to come to rest inside the building.

The structural models, partially shown in Figures 6–6 through 6–9, included:

- Core columns and spliced column connections;
- Floor slabs and beams within the core;
- Exterior columns and spandrels, including the bolted connections between the exterior panels in the refined mesh areas; and
- Tenant space floors, composed of the combined floor slab, metal decking, and steel trusses.

They also included representations of the interior partitions and workstations. The live load mass was distributed between the partitions and cubicle workstations.

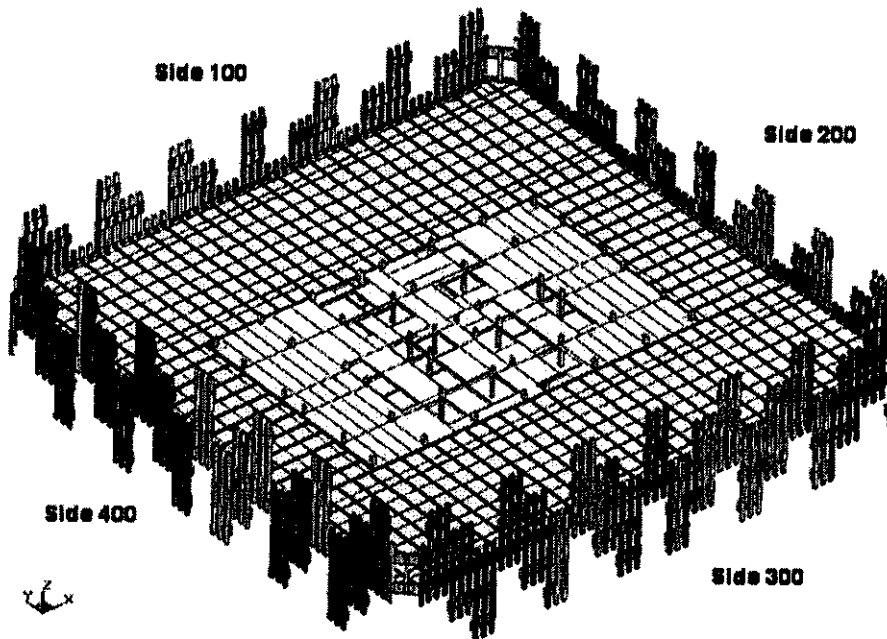


Figure 6-6. Structural model of the 96th floor of WTC 1.

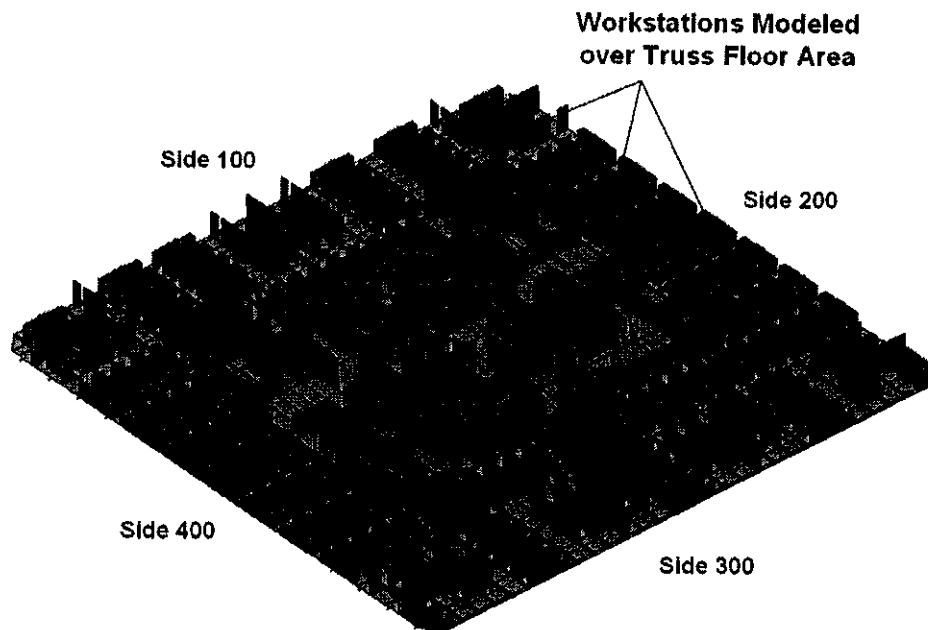


Figure 6-7. Model of the 96th floor of WTC 1, including interior contents and partitions.

Chapter 6

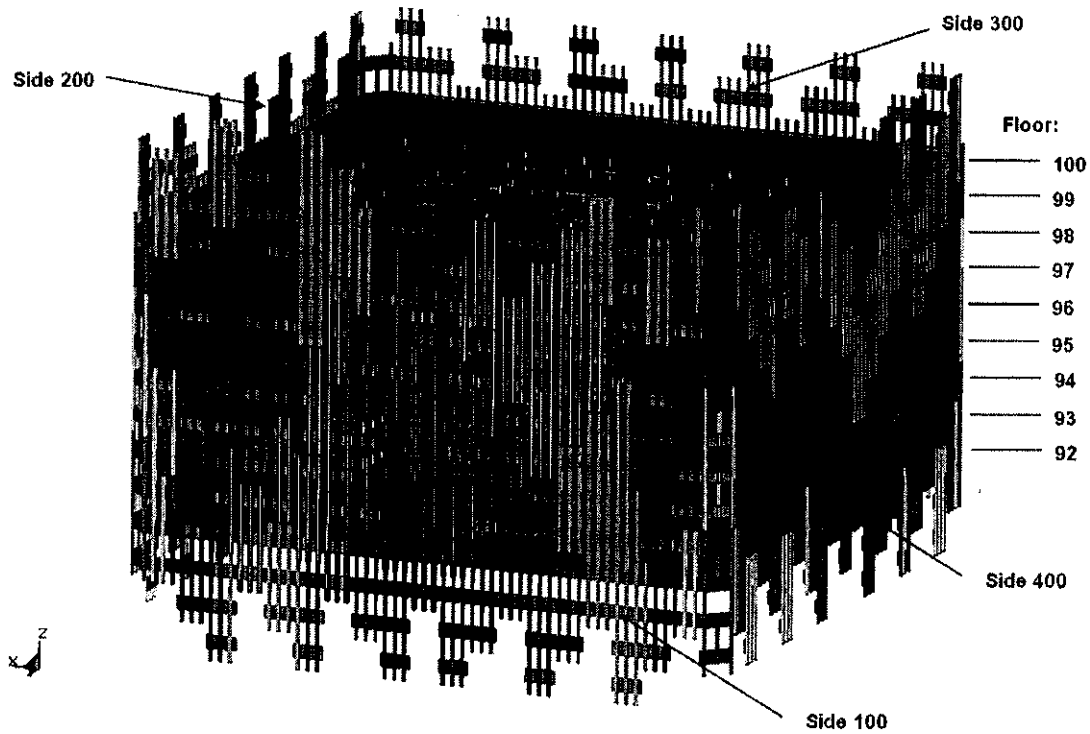


Figure 6-8. Multi-floor global model of WTC 1, viewed from the north.

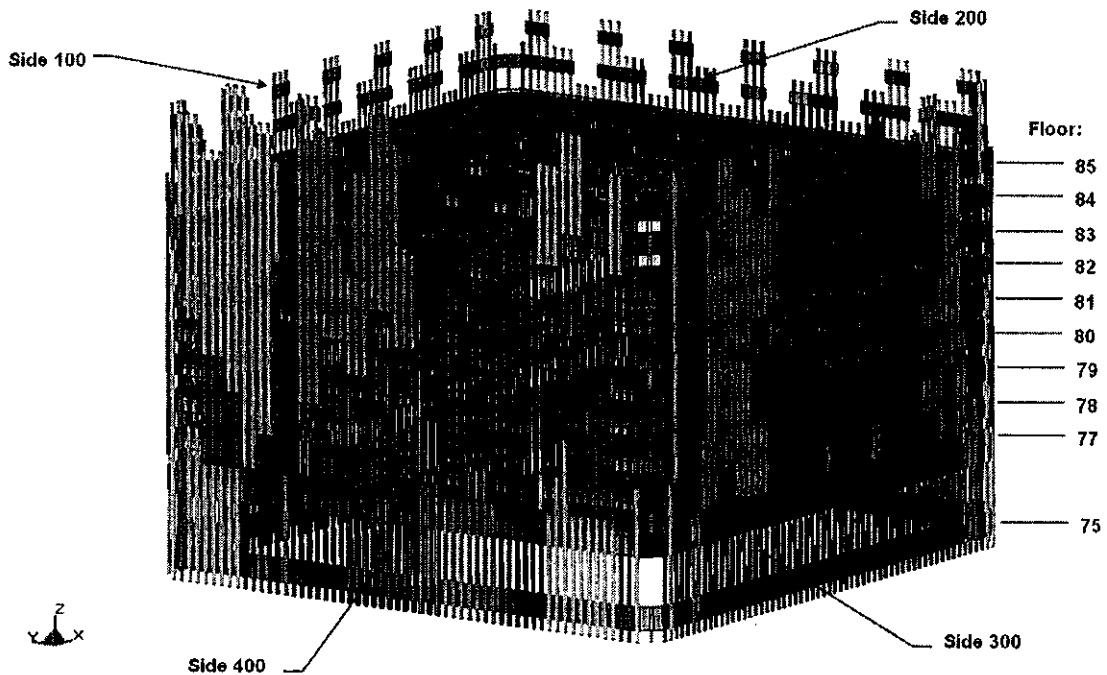


Figure 6-9. Multi-floor global model of WTC 2, viewed from the south.

Within these models, it was critical that the structural and furnishing materials behaved correctly when impacted by the aircraft or debris. For each grade of steel, the stress-strain behavior and the yield strength were represented using data from tests conducted at NIST. The weakening and failure of the concrete floor slabs were simulated using material models embedded in LS-DYNA. The primary influence of the nonstructural components on the impact behavior was their inertial contribution. Values for the resistance to rupture of gypsum panels and the fracture of the wood products in the workstations were obtained from published studies.

In order to complete the global models of the two towers, models of sections of the buildings were developed. As shown in Section 6.8.1, these submodels enabled efficient identification of the principal features of the interaction of the buildings with specific aircraft components.

6.6.4 Building Structural Models for Structural Response to Impact Damage and Fire and Collapse Initiation Analysis

The structural response and collapse analysis of the towers was conducted in three phases by NIST and Simpson Gumpertz & Heger, Inc. (SGH), under contract to NIST. The first phase included component and detailed subsystem models of the floor and exterior wall panels. The objectives of Phase 1 were to gain understanding into the response of the structure under stress and elevated temperatures, identify dominant modes of failure, and develop reductions in modeling complexity that could be applied in Phase 2. The second phase analyzed major subsystem models (the core framing, a single exterior wall, and full tenant floors) to provide insight into their behavior within the WTC global system. The third phase was the analysis of global models of WTC 1 and WTC 2 that took advantage of the knowledge gained from the more detailed and subsystem models. A separate global analysis of each tower helped determine the relative roles of impact damage and fires with respect to structural stability and sequential failures of components and subsystems and was used to determine the probable collapse initiation sequence.

Phase 1: Component and Detailed Subsystem Analyses

Floor Subsystem Analysis

The floors played an important role in the structural response of the WTC towers to the aircraft impact and ensuing fires. Prior to the development of a floor subsystem model, three component analyses were conducted, as follows:

- **Truss seats.** Figure 6-10 shows how an exterior seat connection was represented in the finite element structural model. The component analysis determined that failure could occur at the bolted connection between the bearing angle and the seat angle, and the truss could slip off the seat. Truss seat connection failure from vertical loads was found to be unlikely, since the needed increase in vertical load was unreasonable for temperatures near 600 °C to 700 °C.
- **Knuckles.** The “knuckle” was formed by the extension of the truss diagonals into the concrete slab and provided for composite action of the steel truss and concrete slab. A model was developed to predict the knuckle performance when the truss and concrete slab acted compositely.

Chapter 6

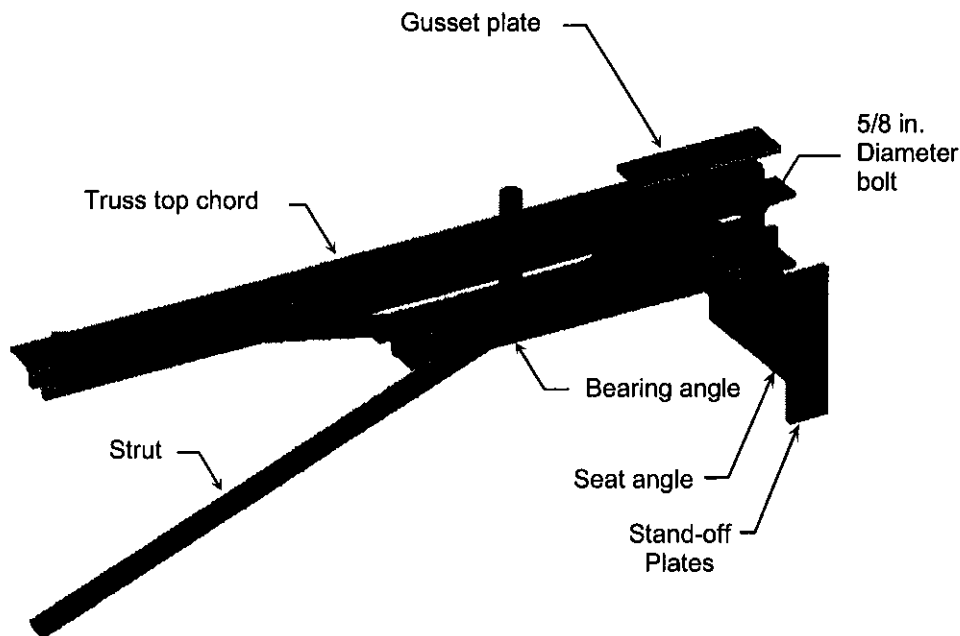


Figure 6-10. Finite element model of an exterior truss seat.

- Single composite truss and concrete slab section. A floor section was modeled to investigate failure modes and sequences of failures under combined gravity and thermal loads. The floor section was heated to 700 °C (with a linear thermal gradient through the slab thickness from 700 °C to 300 °C at the top surface of the slab) over a period of 30 min. Initially the thermal expansion of the floor pushed the columns outward, but with increased temperatures, the floor sagged and the columns were pulled inward. Knuckle failure was found to occur mainly at the ends of the trusses and had little effect on the deflection of the floor system. Figure 6-11 shows that the diagonals at the core (right) end of the truss buckled and caused an increase in the floor system deflection, ultimately reaching approximately 42 in. Two possible failure modes were identified for the floor-truss section: sagging of the floor and loss of truss seat support.

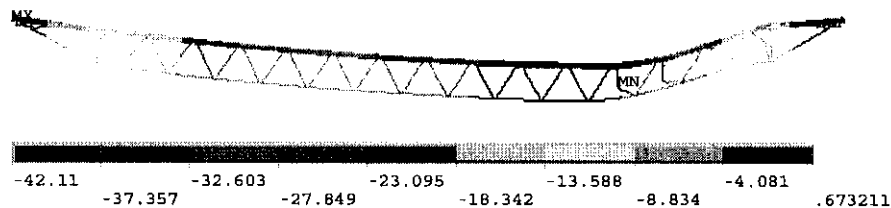


Figure 6-11. Vertical displacement at 700 °C.

A finite element model of the full 96th floor of WTC 1 was translated from the SAP2000 reference models into ANSYS 8.1 for detailed structural evaluation (Figure 6–12)¹⁴. The two models generated comparable predictions of the behavior under dead or gravity loads.

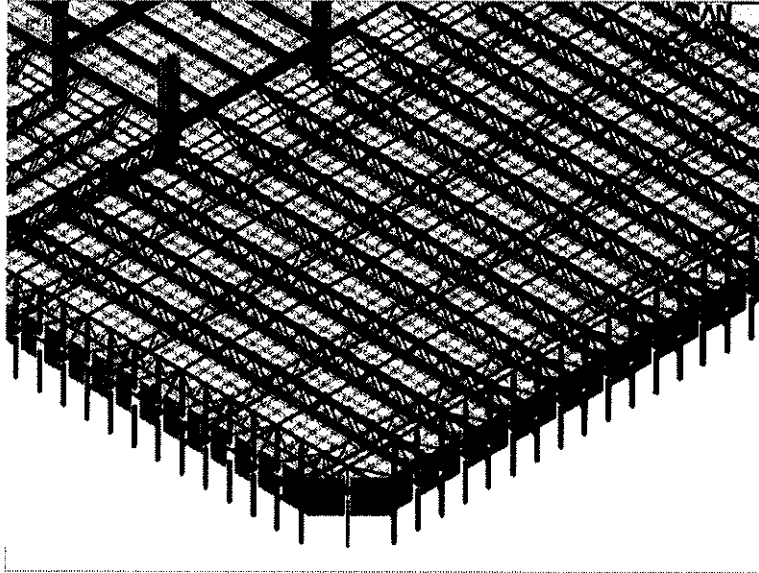


Figure 6–12. ANSYS model of 96th floor of WTC 1.

The model was used to evaluate structural response under dead and live loads and elevated temperatures, identify failure modes and associated temperatures and times to failure, and identify reductions in modeling complexity for global models and analyses. The structural response included thermal expansion of steel and concrete members, temperature-dependent properties of steel and concrete that affected material stiffness and strength, and bowing or buckling of structural members. The deformation and failure modes identified were floor sagging between truss supports, floor sagging resulting from failure of a seat at either end of the truss, and failure of the floor subsystem truss supports.

Exterior Wall Subsystem

The exterior walls played an important role in each tower's reaction to the aircraft impact and the ensuing fires. Photographic and video evidence showed inward bowing of large sections of the exterior walls of both towers just prior to the time of collapse.

A finite element model of a wall section was developed in ANSYS for evaluation of structural response under dead and live loads and elevated structural temperatures, determination of loads that would have caused buckling, and identification of reductions of modeling complexity for global models and analyses. The modeled unit consisted of seven full column/spandrel panels (described in Section 1.2.2) and portions of four other panels. The model was validated against the reference model developed by LERA (Section 6.6.2) by comparing the stiffness for a variety of loading conditions.

¹⁴ ANSYS allowed including the temperature-varying properties of the structural materials, a necessary feature not available in SAP 2000.

Chapter 6

The model was subjected to several gravity loads and heating conditions, several combinations of disconnected floors, and pull-in from sagging floors until the point of instability. In one case, the simulation assumed three disconnected floors, and the top of the wall subsystem was subjected to “push-down” analysis, i.e., an increasing force to provide a measure of remaining capacity in the wall section.

The model captured possible failure modes due large lateral deformations, column buckling from loss of support at floor truss seats and diagonal straps, failure of column splice bolts, and failure of spandrel splice bolts or tearing of spandrel or splice plates at bolt holes. The model also showed:

- Large deformations and buckling of the spandrels could be expected at high temperatures, but they did not significantly affect the stability of the exterior columns and generally did not need to be precisely modeled in the tower models.
- Partial separations of the spandrel splices could be expected at elevated temperatures, but they also did not significantly affect the stability of the exterior columns.
- Exterior column splices could be expected to fail at elevated temperatures and needed to be accurately modeled.
- Plastic buckling of columns, with an ensuing rapid reduction of load, was to be expected at extremely high loads and at low temperatures.
- The sagging of trusses resulted in approximately 14 kip of inward pull per truss seat on the attached perimeter column.

Phase 2: Major Subsystem Analyses

Building on these results, ANSYS models were constructed of each of the three major structural subsystems (core framing, a single exterior wall, and full composite floors) for each of the towers. The models were subjected to the impact damage and elevated temperatures from the fire dynamics and thermal analyses to be described later in this chapter.

Core Framing

The two tower models included the core columns, the floor beams, and the concrete slabs from the impact and fire zones to the highest floor below the hat truss structure: from the 89th floor to the 106th floor for WTC 1 and from the 73rd floor to the 106th floor for WTC 2. Within these floors, aircraft-damaged structural components were removed. Below the lowest floors, springs were used to represent the stiffness of the columns. In the models, the properties of the steel varied with temperature, as described in Section 5.5.2. This allowed for realistic structural changes to occur, such as thermal expansion, buckling, and creep.

The forces applied to the models included gravity loads applied at each floor, post-impact column forces applied at the top of the model at the 106th floor, and temperature histories applied at 10 min intervals with linear ramping between time intervals.

Under these conditions, the investigators first determined the stability of the core under impact conditions and then its response under thermal loads:

- In WTC 1, the core was stable under Case A (base case) impact damage, but the model could not reach a stable solution under Case B (more severe) impact damage.
- The WTC 1 core became unstable under Case A impact damage and Case B thermal loads as it leaned to the northwest (due to insulation dislodged from the northwest corner column); the core model was restrained in horizontal directions at floors above the impact zone half way through the thermal loads.
- The WTC 2 core was stabilized for Case C (base case) by providing horizontal restraint at all floors representing the restraint provided by the perimeter wall to resist leaning to the southeast. A converged, stable solution was not found for Case D (more severe) impact damage.
- The WTC 2 stabilized core model for Case C impact damage was subjected to Case D thermal loads.

Following each simulation, a pushdown analysis was performed to determine the core's reserve capacity. The analysis results showed that:

- The WTC 1 isolated core structure was most weakened from thermal effects at the center of the south side of the core. (Smaller displacements occurred in the global model due to the constraints of the hat truss and floors.)
- The WTC 2 isolated core was most weakened from thermal effects at the southeast corner and along the east side of the core. (Larger displacements occurred in the global model as the isolated core model had lateral restraints imposed that were somewhat stiffer than in the global model.)

Composite Floor

The composite floor model was used to determine the response of a full floor to Case A and B thermal loads for WTC 1 floors and Case C and D thermal loads for WTC 2 floors. It included:

- A reduced complexity truss model, validated against the single truss model results.
- Primary and bridging trusses, deck support angles, spandrels, core floor beams, and a concrete floor slab.
- Fire-generated local temperature histories applied at 10 min intervals with linear ramping between time intervals.
- Temperature-dependent concrete and steel properties, except for creep behavior.

Chapter 6

- Restraint provided by exterior and core columns, which extended one floor above and below the modeled floor. The potential for large deflections and buckling of individual structural members and the floor system were included.

The results showed that:

- At lower elevated temperatures (approximately 100 °C to 400 °C), the floors thermally expanded and displaced the exterior columns outward by a few inches; horizontal displacement of the core columns was insignificant. None of the floors buckled as they thermally expanded, even with the exterior columns restrained so that no horizontal movement was allowed at the floors above and below the heated floor, which maximized column resistance to floor expansion. Even with this level of column restraint, the exterior columns did not develop a sufficient reaction force (push inward to resist the expansion outward) to buckle any of the floors.
- At higher elevated temperatures (above 400 °C), the floors began to sag as the floors' stiffness and strength were reduced with increasing temperature, and the difference in thermal expansion between the trusses and the concrete slab became larger. As the floor sagging increased, the outward displacement of the exterior columns was overcome, and the floors exerted an inward pull force on the exterior columns.
- Floor sagging was caused primarily by either buckling of truss web diagonals or disconnection of truss seats at the exterior wall or the core perimeter. Except for the truss seat failures near the southeast corner of the core in WTC 2 following the aircraft impact, web buckling or truss seat failure was caused primarily by elevated temperatures of the structural components.
- Analysis results from the detailed truss model found that the floors began to exert inward pull forces when floor sagging exceeded approximately 25 in. for the 60 ft floor span.
- Sagging at the floor edge was due to loss of vertical support at the truss seats. The loss of vertical support was caused in most cases by the reduction in vertical shear capacity of the truss seats due to elevated steel temperatures.
- Case B impact damage and thermal loads for WTC 1 floors resulted in floor sagging on the south side of the tower over floors that reasonably matched the location of inward bowing observed on the south face. Case A impact damage and thermal loads did not result in sagging on the south side of the floors.
- Cases C and D impact damage and thermal loads for WTC 2 both resulted in floor sagging on the east side of the tower over floors that reasonably matched the location of inward bowing observed on the east face. However, Case D provided a better match.

Exterior Wall

Exterior wall models were developed for the south face of WTC 1 (floors 89 to 106) and the east face of WTC 2 (floors 73 to 90). These sections were selected based on photographic evidence of column bowing.

Many of the simulation conditions were similar to those for the isolated core modeling: removal of aircraft-damaged structural components, representation of lower floors by springs, temperature-varying steel properties, gravity loads applied at each floor, post-impact column forces applied at the 106th floor, and temperature histories applied at 10 min intervals with linear ramping between time intervals.

The analysis results showed that:

- Inward pull forces were required to produce inward bowing consistent with the displacements measured from photographs. The inward pull was caused by sagging of the floors. Heating of the inside faces of the exterior columns also contributed to inward bowing.
- Exterior wall sections bowed outward in a pushdown analysis when several consecutive floors were disconnected, the interior face of the columns was heated, and column gravity loads increased (e.g., due to load redistribution from the core and hat truss). At lower temperatures, thermal expansion of the inside face was insufficient to result in inward bowing of the entire exterior column. At higher temperatures, outward bowing resulted from the combined effects of reduced steel strength on the heated inside face, which shortened first under column gravity loads, and the lack of lateral restraint from the floors.
- The observed inward bowing of the exterior wall indicated that most of the floor connections must have been intact to cause the observed bowing.
- The extent of floor sagging observed at each floor was greater than that predicted by the full floor models. The estimates of the extent of sagging at each floor was governed by the combined effects of insulation damage and fire; insulation damage estimates were limited to areas subject to direct debris impact. Other sources of floor and insulation damage from the aircraft impact and fires (e.g., insulation damage due to shock and subsequent vibrations as a result of aircraft impact or concrete slab cracking and spalling as a result of thermal effects) were not included in the floor models.
- Case B impact damage and thermal loads for the WTC 1 south wall, combined with pull-in forces from floor sagging, resulted in an inward bowing of the south face that reasonably matched the observed bowing. The lack of floor sagging for the Case A impact damage and thermal loads resulted in no inward bowing for the south face.
- Cases D impact damage and thermal loads for the WTC 2 east wall, combined with pull-in forces from floor sagging, resulted in an inward bowing of the east face that reasonably matched the observed bowing.

Chapter 6

Phase 3: Global Modeling

The global models were used for the two final simulations and provided complete analysis of results and insight into the subsystem interactions leading to the probable collapse sequence. Based upon the results of the major subsystem analyses, impact damage and thermal loads for Cases B and D were used for WTC 1 and WTC 2, respectively. The models extended from floor 91 for WTC 1 and floor 77 for WTC 2 to the roof level in both towers. Although the renditions of the structural components had been reduced in complexity while maintaining essential nonlinear behaviors, based on the findings from the component and subsystem modeling, the global models included many of the features of the subsystem models:

- Removal of aircraft-damaged structural components.
- Application of gravity loads following removal of aircraft damaged components and prior to thermal loading.
- Temperature-dependent concrete and steel properties.
- Creep strains for column components.
- Representation of lower floors by springs.
- Local temperature histories applied at 10 min intervals with linear ramping between time intervals.

There were several adjustments to the models based on the findings from the subsystem modeling:

- Removal of thermal expansion from the spandrels and equivalent slabs in the tenant area to avoid local buckling that affected convergence but had little influence on global collapse initiation.
- Representing the WTC 2 structure above the 86th floor as a single “super-element” to reduce model complexity. The floors above the impact zone had only exhibited linear behavior in the previous analyses. This modification assumed linear behavior of the hat truss, which was checked as part of the review of analysis results.
- Representation of the lower part of the tower (starting several floors below the impact damage) as a super-element. This prevented the use of construction sequence in applying gravity loads to the model (where loads are applied in stages to simulate the construction of the building). The lack of construction sequence increased the forces on the exterior columns slightly, and decreased those on the core columns slightly.

The inclusions of creep for column components was necessary for the accuracy of the models, but its addition also greatly increased the computation time. As a result, the simulations of WTC 1 took 22 days and those of WTC 2 took 14 days on a high-end computer workstation. The results of these simulations are presented in Section 6.14.

6.7 THE AIRCRAFT STRUCTURAL MODEL

Due to their similarity, the two Boeing 767-200ER aircraft were represented by a single, finite element model, two views of which are shown in Figure 6-13. The model consisted of about 800,000 elements. The typical element dimensions were between 1 in. and 2 in. for small components, such as spar or rib flanges, and 3 in. to 4 in. for large parts such as the wing or fuselage skin. Structural data on which to base the model were collected from the open literature, electronic surface models and CAD drawings, an inspection of a 767-300ER, Pratt and Whitney Engine Reference Manuals, American Airlines and United Airlines, and the Boeing Company website.

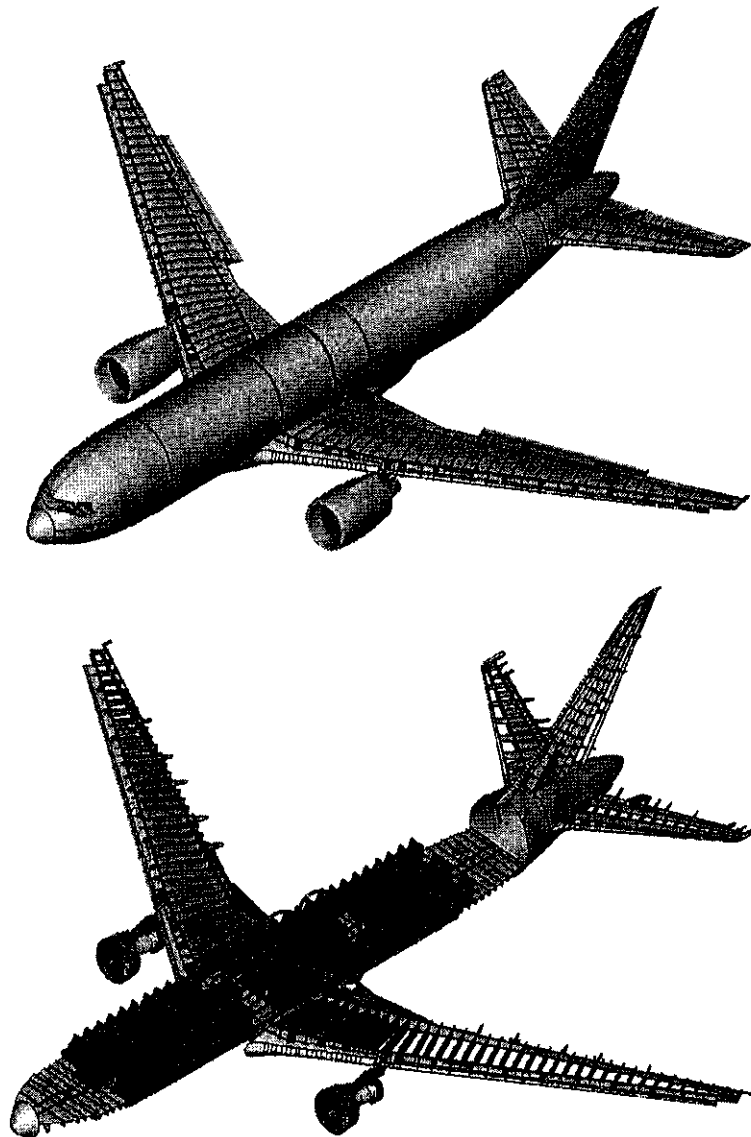


Figure 6-13. Finite element model of the Boeing 767-200ER.

Chapter 6

More detailed models of subsections of the aircraft were constructed for the component level analyses described below. Special emphasis was placed on modeling the aircraft engines, due to their potential to produce significant damage to the tower components. The element dimensions were generally between 1 in. and 2 in., although even smaller dimensions were required to capture some details of the engine geometry. The various components of the resulting engine model are shown in Figure 6-14. Fuel was distributed in the wing as shown in Figure 6-15 based on a detailed analysis of the fuel distribution at the time of impact.

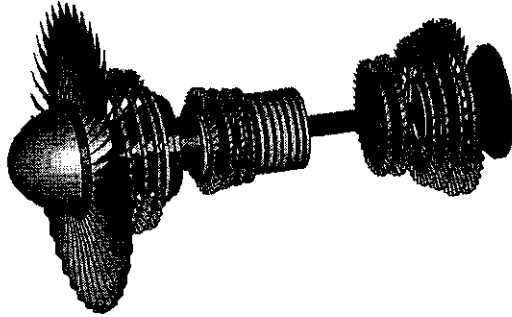


Figure 6-14. Pratt & Whitney PW4000 turbofan engine model.

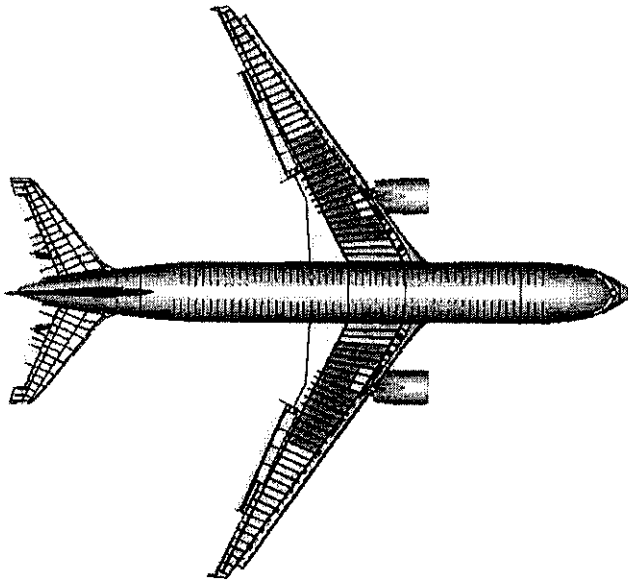


Figure 6-15. Boeing 767-200ER showing the jet fuel distribution at time of impact.

6.8 AIRCRAFT IMPACT MODELING

6.8.1 Component Level Analyses

Prior to conducting the full simulations of the aircraft impacting the towers, a series of smaller scale simulations was performed to develop understanding of how the aircraft and tower components fragmented and to develop the simulation techniques required for the final computations. These simulations began with finely meshed models of key components of the tower and aircraft structures and progressed to relatively coarsely meshed representations that could be used in the global models. Examples of these component-level analyses included impact of a segment of an aircraft wing with an exterior column, impact of an aircraft engine with exterior wall panels, and impact of a fuel-filled wing segment with exterior wall panels.

Figure 6–16 shows two frames from the last of these analyses, with the wing segment entering from the left, being fragmented as it penetrates the exterior columns, and spraying jet fuel downstream.

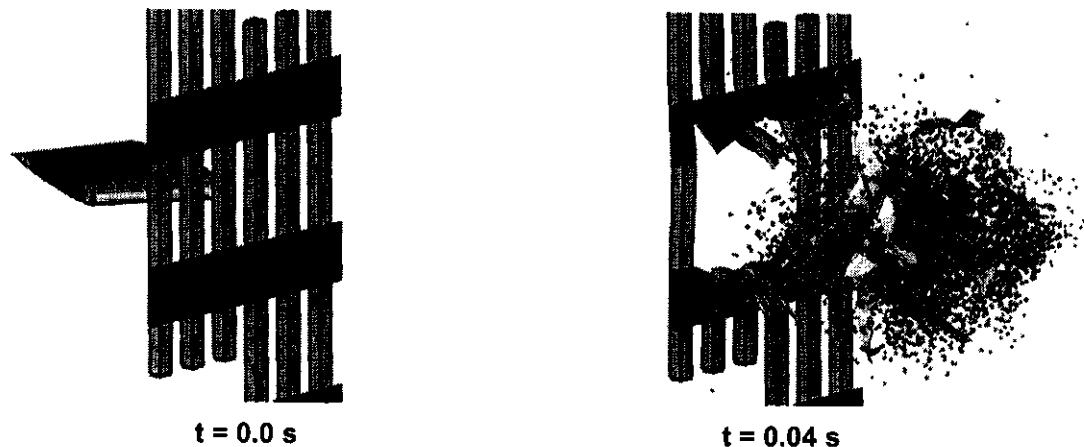


Figure 6–16. Calculated impact on an exterior wall by a fuel-laden wing section.

The Investigation Team gained valuable knowledge from these component impact analyses, for example:

- Moving at 500 mph, an engine broke any exterior column it hit. If the engine missed the floor slab, the majority of the engine core remained intact and had enough residual momentum to sever a core column upon direct impact.
- The impact of the inner half of an empty wing significantly damaged exterior columns but did not result in their complete failure. Impact of the same wing section, but filled with fuel, did result in failure of the exterior columns.

Chapter 6

6.8.2 Subassembly Impact Analyses

Next, a series of simulations were performed for intermediate-sized sections of a tower. These subassembly analyses investigated different modeling techniques and associated model sizes, run times, numerical stability, and impact response. Six simulations were performed of an aircraft engine impacting a subassembly that included structural components from the impact zone on the north face of WTC 1, exterior panels, truss floor structures, core framing, and interior contents (workstations). One response of the structure to the engine impact is shown in Figure 6-17.

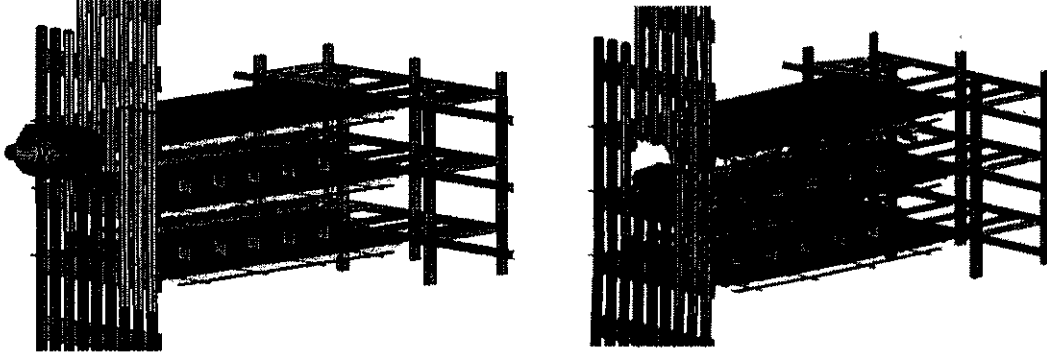


Figure 6-17. Response of a tower subassembly model to engine impact.

Typical knowledge gained from these simulations were:

- The mass of the concrete floor slab and nonstructural contents had a greater effect on the engine deceleration and subsequent damage than did the concrete strength.
- Variation of the failure criteria of the welds in the exterior columns did not result in any noticeable difference in the damage pattern or the energy absorbed by the exterior panels.

6.8.3 Aircraft Impact Conditions

From the NIST photographic and video collection, the speed and orientation of the aircraft (Table 6-4) were estimated at the time of impact. The geometry of the wings, different in flight from that at rest, was estimated from the impact pattern in the photographs and the damage documented on the exterior panels by NIST. United Airlines and American Airlines provided information on the contents of the aircraft, the mass of jet fuel, and the location of the fuel within the wing tanks.

Table 6-4. Summary of aircraft impact conditions.

Condition	AA 11 (WTC 1)	UAL 175 (WTC 2)
Impact Speed (mph)	443 ± 30	542 ± 24
Vertical Approach Angle	10.6° ± 3° below horizontal (heading downward)	6° ± 2° below horizontal (heading downward)
Lateral Approach Angle	180.3° ± 4° clockwise from Plan North ^a	13° ± 2° clockwise from Plan North ^a
Roll Angle (left wing downward)	25° ± 2°	38° ± 2°

a. Plan North is approximately 29 degrees clockwise from True North.

6.8.4 Global Impact Analysis

From the component and subassembly simulations, it became apparent that each computation of the full tower and aircraft would take weeks. Furthermore, the magnitude and location of damage to the tower structure were sensitive to a large number of initial conditions, to assumptions in the representation of the collision physics, and to any approximations in the numerical methods used to solve the physics equations. Thus, it was necessary to choose a manageable list of the factors that most influenced the outcome of a simulation. Careful screening was conducted at the component and subassembly levels, leading to identification of the following prime factors:

- Impact speed,
- Vertical approach angle of the aircraft,
- Lateral approach angle of the aircraft,
- Total aircraft weight,
- Aircraft materials failure strain,
- Tower materials failure strain, and
- Building contents weight and strength.

Guided by these results and several preliminary global simulations, two global simulations were selected for inclusion in the four-step simulation of the response of each tower, as described in Section 6.1. The conditions for these four runs are shown in Table 6–5. The computers simulate the aircraft flying into the tower, calculated the fragments that were formed from both the aircraft and the building itself, and then followed the fragments. The jet fuel, atomized upon impact into about 60,000 “blobs” averaging one pound, dispersed within and outside the building. Each simulation continued until the debris motion had reduced to a level that was not expected to produce any significant further impact damage.

Table 6–5. Input parameters for global impact analyses.

Analysis Parameters		WTC 1		WTC 2	
		Case A	Case B	Case C	Case D
Flight Parameters	Impact Speed	443 mph	472 mph	542 mph	570 mph
	Vertical Approach Angle	10.6°	7.6°	6.0°	5.0°
	Lateral Approach Angle	180.0°	180.0°	13.0°	13.0°
Aircraft Parameters	Weight	100 %	105 %	100 %	105 %
	Failure Strain	100 %	125 %	100 %	115 %
Tower Parameters	Failure Strain	100 %	80 %	100 %	90 %
	Live Load Weight ^a	25 %	20 %	25 %	20 %
	Contents Strength	100 %	100 %	100 %	80 %

a. Live load weight expressed as a percentage of the design live load.

Chapter 6

These simulations each took about 2 weeks on a 12-node computer cluster. Figure 6–18 shows six frames from the animation of one such simulation.

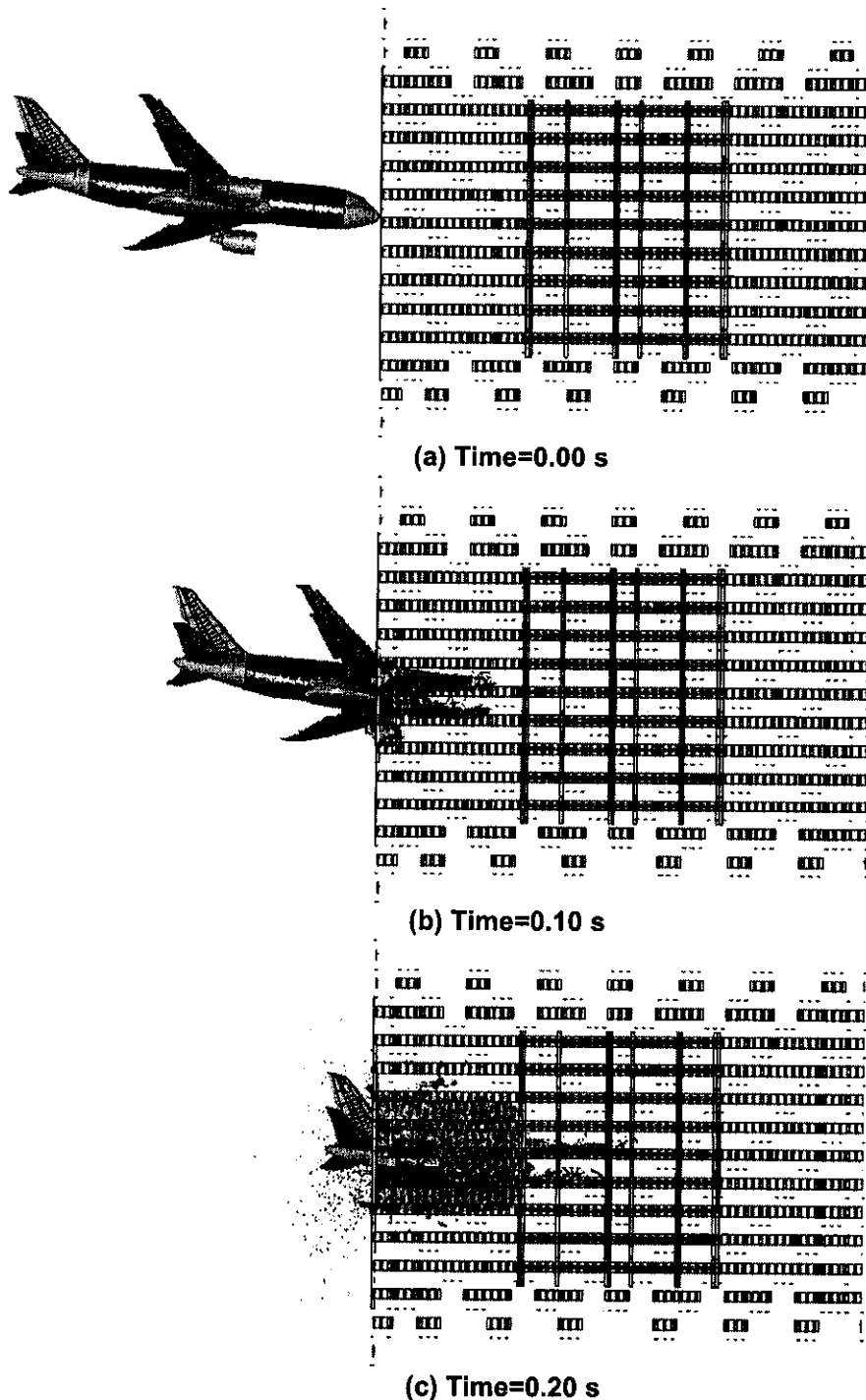
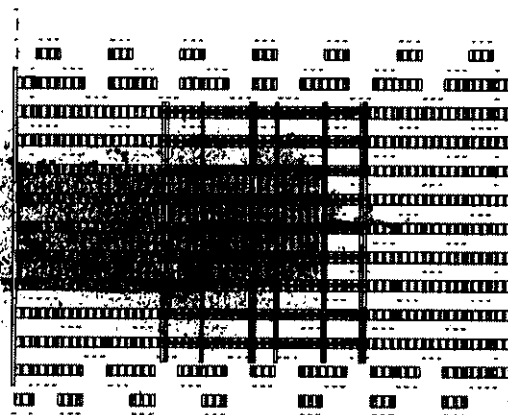
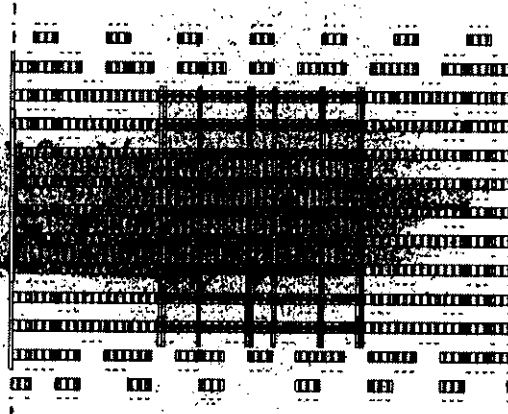


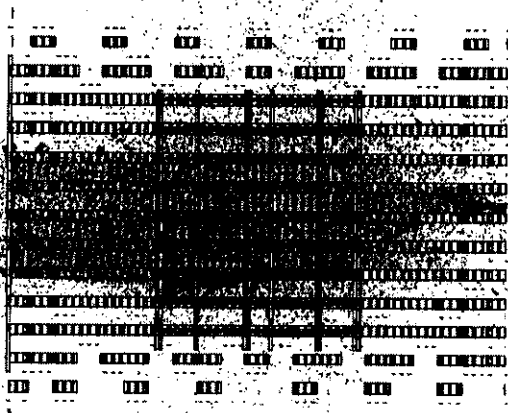
Figure 6–18. Side view of simulated aircraft impact into WTC 1, Case B.



(d) Time=0.30 s



(e) Time=0.40 s



(f) Time=0.50 s

Figure 6–18. Side view of simulated aircraft impact into WTC 1, Case B (Cont.)

6.9 AIRCRAFT IMPACT DAMAGE ESTIMATES

6.9.1 Structural and Contents Damage

Each of the four global simulations generated information about the state of the structural components following the impact of the aircraft. The four degrees of column damage are defined as follows and shown graphically in Figure 6–19. The unstrained areas are blue and the highly strained areas are red.

- Lightly damaged column: column impacted, but without significant structural deformation;
- Moderately damaged column: visible local distortion, but no deformation of the column centerline;
- Heavily damaged column: Permanent deflection of the column centerline; and
- Failed column: Column severed.

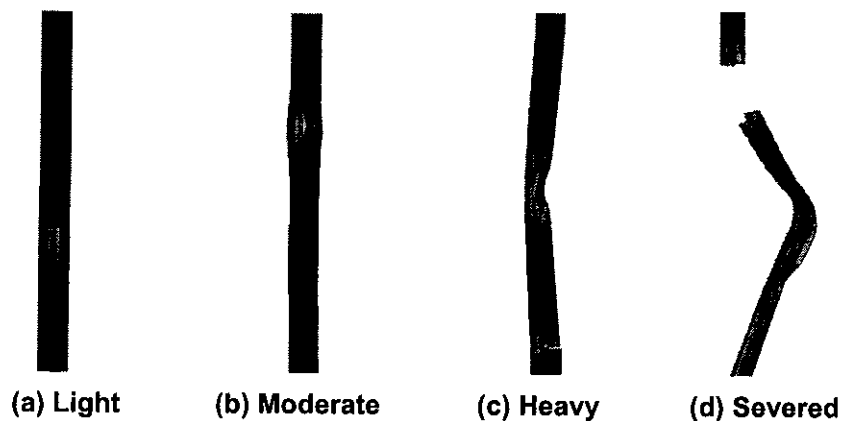


Figure 6–19. Column damage levels.

Figure 6–20 shows the calculated damage to a floor slab. Figure 6–21 shows the response of the furnishings and the jet fuel to the impact. Figures 6–22 through 6–25 show the combined damage for all floors for the four global simulations. The latter proved useful in visualizing the extent of aircraft impact in one graphic image.

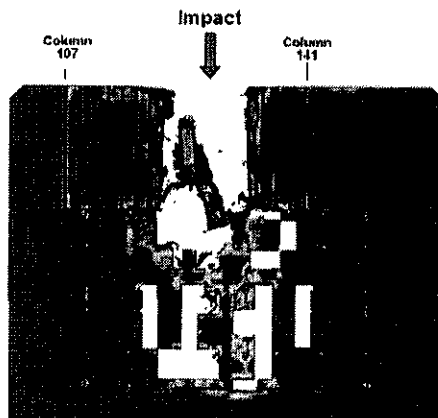
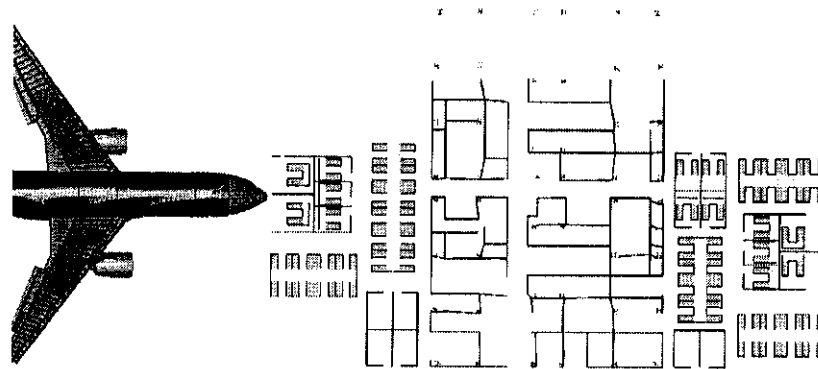
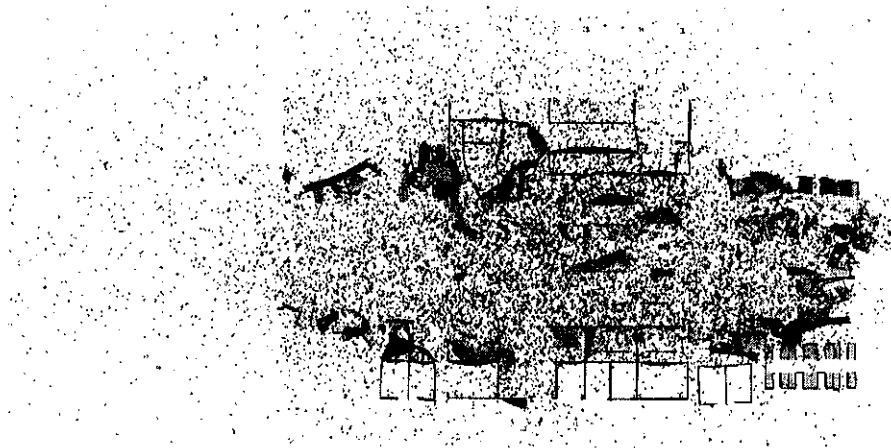


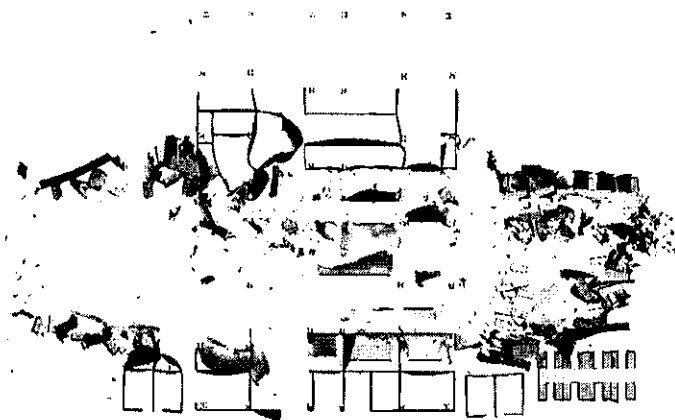
Figure 6–20. Case B damage to the slab of floor 96 of WTC 1.



(a) Pre-impact configuration



(b) Calculated impact response



(c) Calculated impact response (fuel removed)

Figure 6–21. Case B simulation of response of contents of 96th floor of WTC 1.

Chapter 6



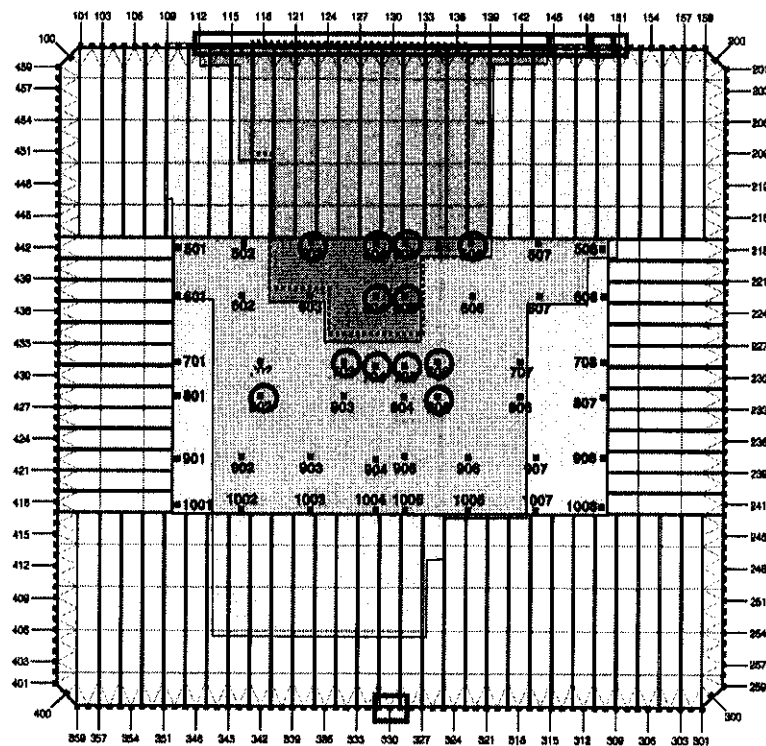
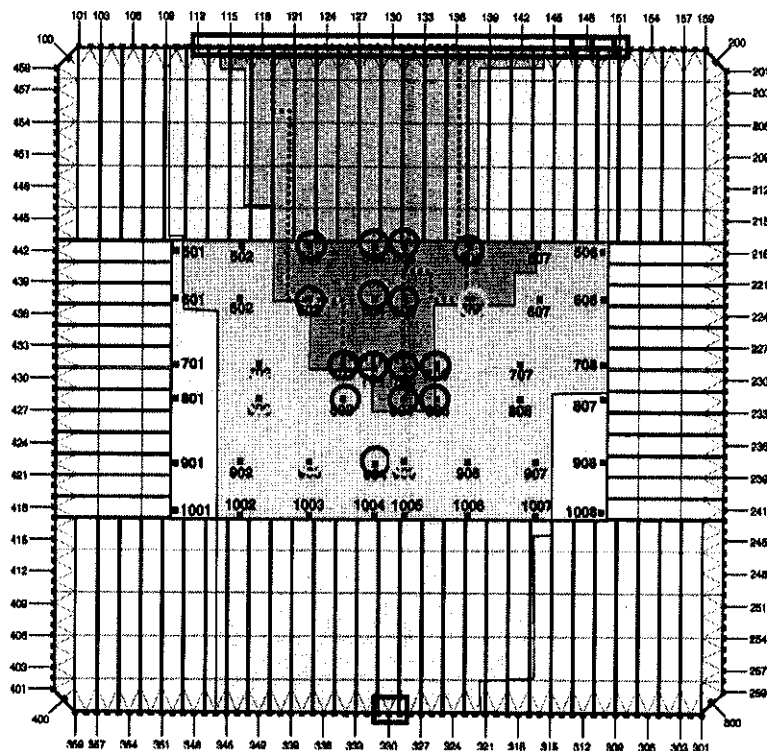
Severe Floor DamageFloor fireproofing Floor system structural damage Floor system removed **Column Damage**Severed Heavy damage Moderate damage Light damage 

Figure 6-22. Combined structural damage to the floors and columns of WTC 1, Case A.

Figure 6-23. Combined structural damage to the floors and columns of WTC 1, Case B.



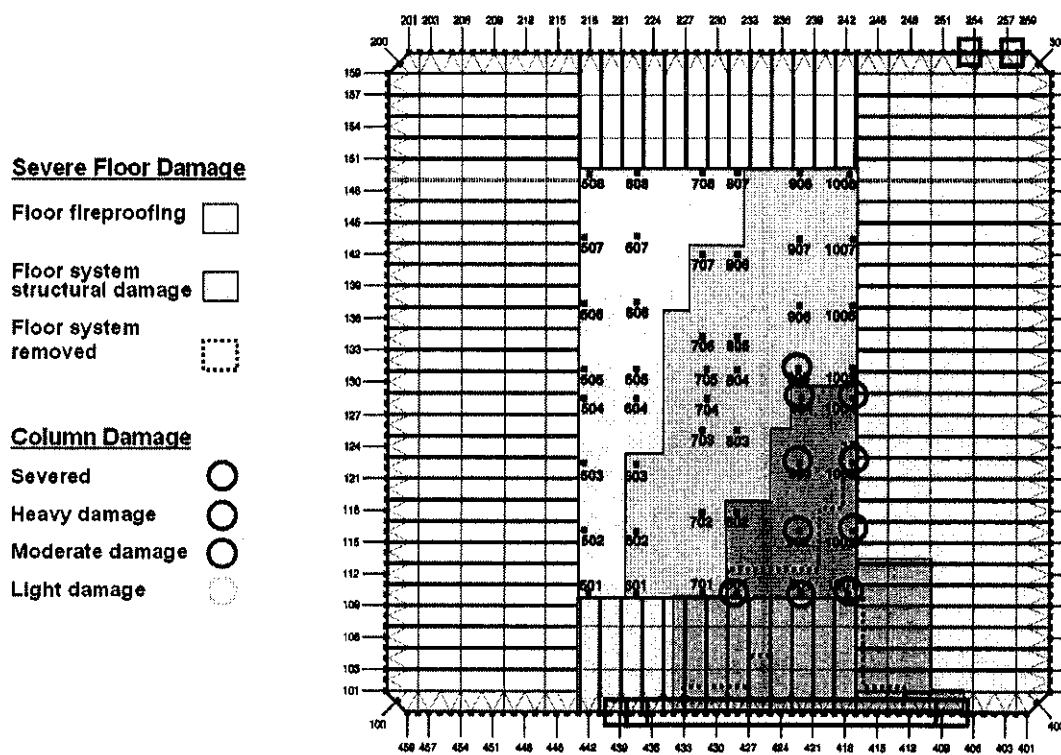
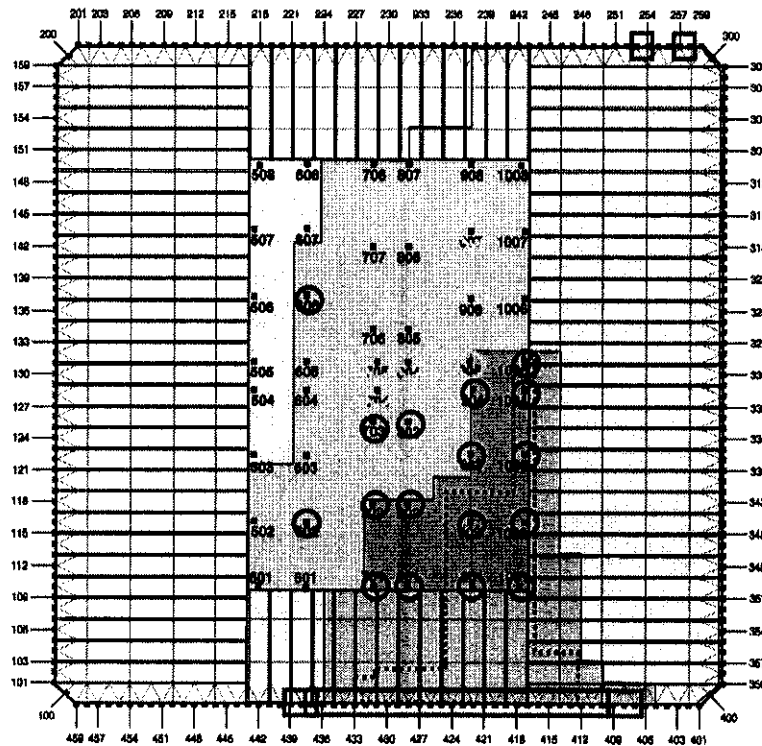


Figure 6-24. Combined structural damage to the floors and columns of WTC 2, Case C.

Figure 6-25. Combined structural damage to the floors and columns of WTC 2, Case D.



6.9.2 Validity of Impact Simulations

Assessment of the aircraft impact simulations of exterior damage to the towers involved comparing the predicted perimeter wall damage near the impact zone with post-impact photographs of the walls. Figure 6-26 shows a photograph of the north face of WTC 1 after impact and the results of the Case A simulation. The calculated silhouettes capture both the position and shape of the actual damage.

Figures 6-27 and 6-28 depict more detailed comparisons between the observed and calculated damage. The aircraft hole is shown in white. The colored dots characterize the mode in which the steel or connection failed (e.g., severed bolt, ripped weld) and the magnitude of the deformation of the steel:

- Green: proper match of failure mode and magnitude
- Yellow: proper match in the failure mode, but not the magnitude
- Red: neither the failure mode nor the magnitude matched
- Black: the observed damage was obscured by smoke, fire, or other factors

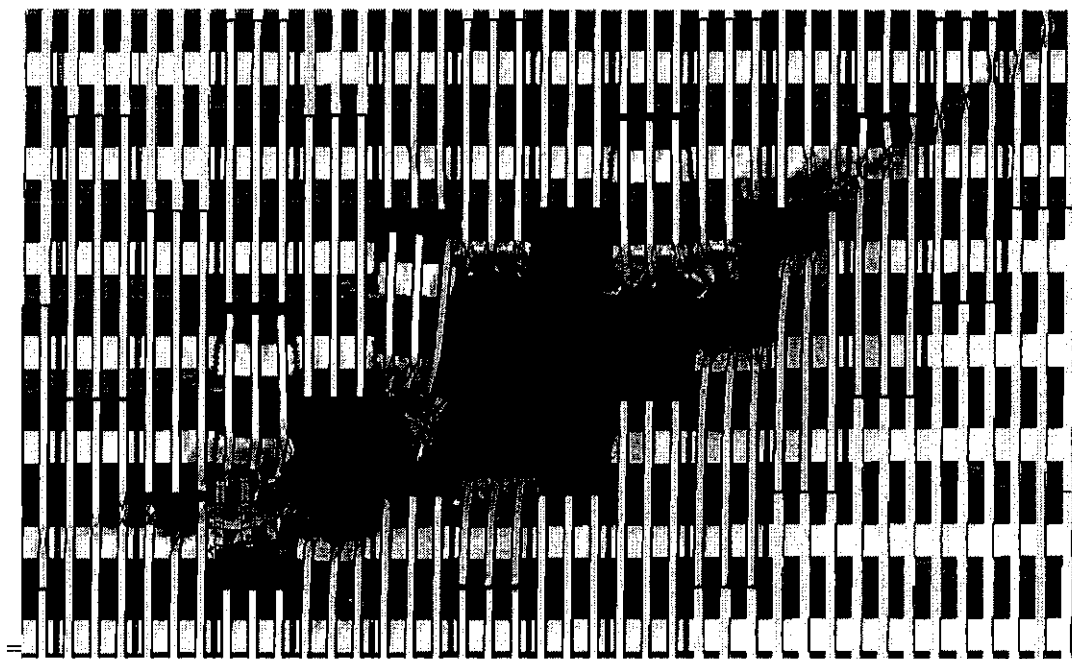
The predominance of green dots and the scarcity of red dots indicate that the overall agreement with the observed damage was very good. The agreement for Cases B and D was slightly lower.

Assessment of the accuracy of the predictions of damage inside the buildings was more difficult, as NIST could not locate any interior photographs near the impact zones. Three comparisons were made:

- The Case A simulation for WTC 1 predicted that the walls of all three stairwells would have been collapsed. This agreed with the observations of the building occupants. The Case A simulation for WTC 2 showed that the walls of stairwell B would have been damaged, but that Stairwell A would have been unaffected. Stairwell C was not included in the WTC 2 model, but is adjacent to where damage occurred. The building occupants reported that Stairwells B and C were impassable; Stairwell A was damaged but passable.
- The two simulations of WTC 2 showed accumulations of furnishings and debris in the northeast corner of the 80th and 81st floors. These piles were observed in photographs and videos.
- Two pieces of landing gear penetrated WTC 1 and landed to the south of the tower. The Case B prediction showed landing gear penetrating the building core, but stopping before reaching the south exterior wall. For WTC 2, a landing gear fragment and the starboard engine penetrated the building and landed to the south. The Case D prediction correctly showed the main landing gear emerging from the northeast corner of WTC 2. However, Case D showed that engine not quite penetrating the building. Minor modifications to the model (all within the uncertainty of the input data) would have resulted in the engine passing through the north exterior wall of the tower.



(a) Observed Damage



(b) Calculated damage

Figure 6-26. Observed and Case A calculated damage to the north face of WTC 1.

Chapter 6

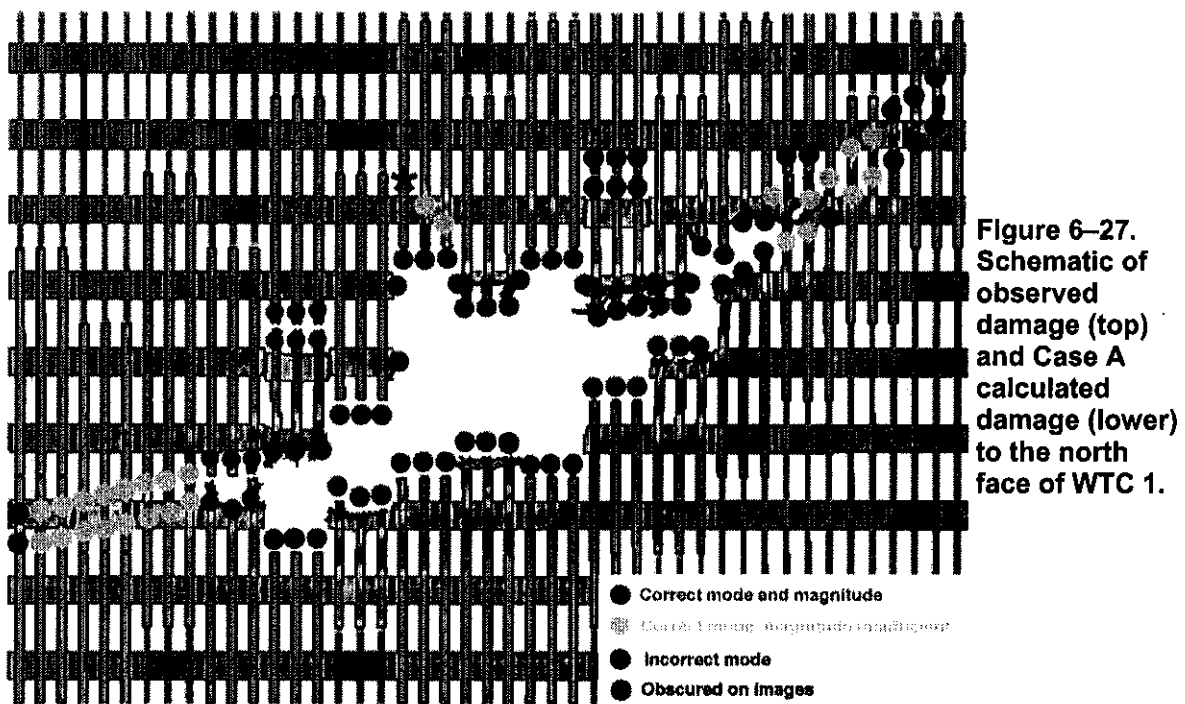
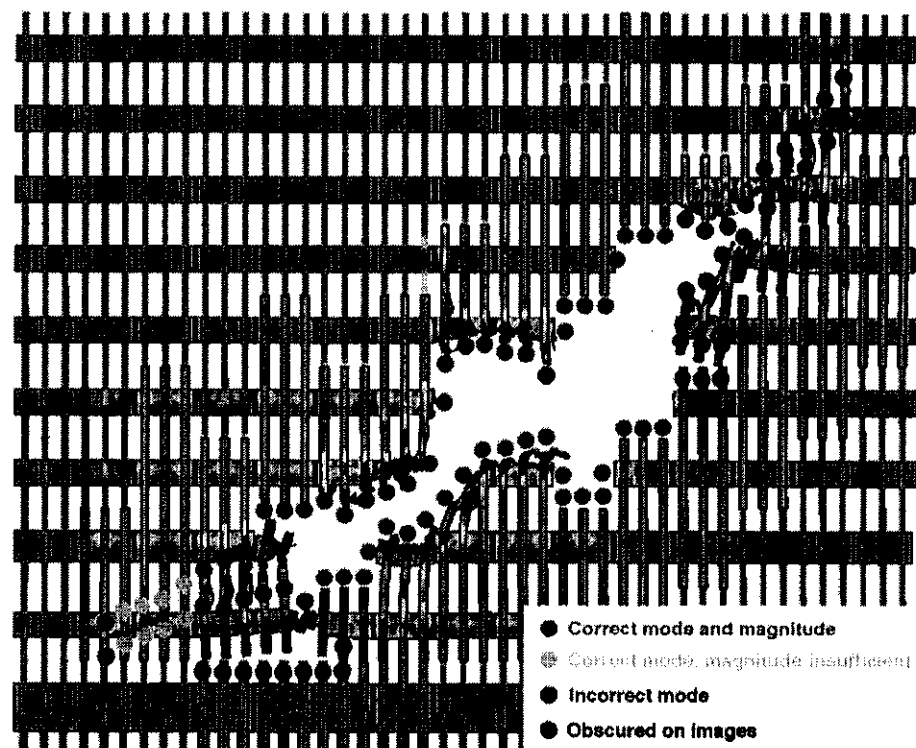


Figure 6-28. Schematic of observed damage (above) and Case C calculated damage (right) to the south face of WTC 2.



Not all of the observables were closely matched by the simulations due to the uncertainties in exact impact conditions, the imperfect knowledge of the interior tower contents, the chaotic behavior of the aircraft breakup and subsequent debris motion, and the limitations of the models. In general, however, the results of the simulations matched these observables sufficiently well that the Investigation Team could rely on the predicted trends.

Simulations of the damage to the core columns had been performed previously by staff of Weidlinger Associates, Inc. (WAI) and the Massachusetts Institute of Technology (MIT). Each developed a range of numbers of failed and damaged columns, as did NIST. The range of the MIT results straddled the NIST results. WAI's analysis resulted in more failed and damaged columns, with WTC 2 being unstable immediately following impact.

6.9.3 Damage to Thermal Insulation

The dislodgement of thermal insulation from structural members could have occurred as a result of (a) direct impact by debris and (b) inertial forces due to vibration of structural members as a result of the aircraft impact. The debris from the aircraft impact included the fragments that were formed from both the aircraft (including the contents and fuel) and the building (structural members, walls, and furnishings). In interpreting the output of the aircraft impact simulations, NIST assumed that the debris impact dislodged insulation if the debris force was strong enough to break a gypsum board partition immediately in front of the structural component. Experiments at NIST confirmed that an array of 0.3 in. diameter pellets traveling at approximately 350 mph stripped the insulation from steel bars like those used in the WTC trusses.

Determining the adherence of SFRM outside the debris zones was more difficult. There was photographic evidence that some fraction of the SFRM was dislodged from perimeter columns not directly impacted by debris.

NIST developed a simple model to estimate the range of accelerations that might dislodge the SFRM from the structural steel components. As the SFRM in the towers was being upgraded with BLAZE-SHIELD II in the 1990s, The Port Authority had measured the insulation bond strength (force required to pull the insulation from the steel). The model used these data as input to some basic physics equations. The resulting ranges of accelerations depended on the geometry of the coated steel component and the SFRM thickness, density and bond strength. For a flat surface (as on the surface of a column), the range was from 20g to 530g, where g is the gravitational acceleration. For an encased bar (such as used in the WTC trusses), the range was from 40g to 730g. NIST estimated accelerations from the aircraft impacts of approximately 100g.

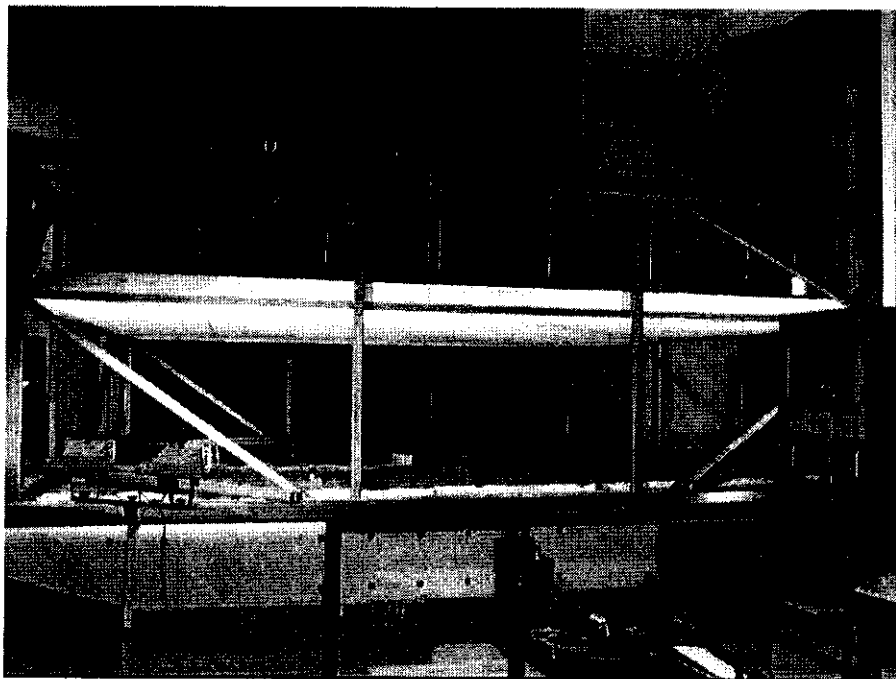
In determining the extent of insulation damage in each tower, NIST only assumed damage where dislodgement criteria could be established and supported through observations or analysis. Thus, NIST made the conservative assumption that insulation was removed only where direct debris impact occurred and did not include the possibility of insulation damage or dislodgement from structural vibration. This assumption produced a lower bound on the bared steel surface area, thereby making it more difficult to heat the steel to the point of failure.

Chapter 6

6.9.4 Damage to Ceiling System

The aircraft impact modeling did not include the ceiling tile systems. To estimate whether the tiles would survive the aircraft impact, the University at Buffalo, under contract to NIST, conducted tests of WTC-like ceiling tile systems using their shake table (Figure 6–29) and impulses related to those induced by the aircraft impact on the towers. The data indicated that accelerations of approximately 5g would most likely result in substantial displacement of ceiling tiles. Given the estimated impact accelerations of approximately 100g, NIST assumed that the ceiling tiles in the impact and fire zones were fully dislodged. This was consistent with the multiple reports of severely damaged ceilings (Chapter 7).

An intact ceiling tile system could have provided the floor trusses with approximately 10 min to 15 min of thermal protection from ceiling air temperatures near 1,000 °C. These temperatures would quickly heat steel without thermal insulation to temperatures for reduction of the strength of structural steels.



Source: NIST

Figure 6–29. Ceiling tile system mounted on the shaking table.

6.9.5 Damage to Interior Walls and Furnishings

As shown in Figure 6–18, the aircraft impact simulations explicitly included the fracture of walls in the debris path and the “bulldozing” of furnishings. Damage to the impacted furnishings was not modeled. Walls and furnishings outside the debris paths were undamaged in the simulations.

6.10 THERMAL ENVIRONMENT MODELING

6.10.1 Need for Simulation

Following the impact of the aircraft, the jet-fuel-ignited fires created the sustained and elevated temperatures that heated the remaining building structure to the point of collapse initiation. The photographic evidence provided some information regarding the locations and spreading of the fires. However, the cameras could only see the periphery of the building interior. The steep viewing angles of nearly all of the photographs and videos further limited the depth of the building interior for which fire information could be obtained. NIST could not locate any photographic evidence regarding the fire exposure of the building core or the floor assemblies.

The simulations of the fires were the second computational step in the identification of the probable sequences leading to the collapse of the towers. The required output of these simulations was a set of three-dimensional, time varying renditions of the thermal and radiative environment to which the structural members in the towers were subjected from the time of aircraft impact until the onset of building collapse. The rigor of the Investigation placed certain requirements on the computational tool (model) used to generate these renditions:

- Resolution of the varying thermal environment across key dimensions, e.g., the truss space;
- Representation of the complex combustibles;
- Computation of flame spread across the large expanses of the WTC floors; and
- Confidence in the accuracy of the predictions.

6.10.2 Modeling Approach

The time frame of the Investigation and the above requirements led to the use of the Fire Dynamics Simulator (FDS). Under development at NIST since 1978, FDS was first publicly released in February 2000 and had been used worldwide on a wide variety of applications, ranging from sprinkler activation to residential and industrial fire reconstructions. However, it had never before been applied to spreading fires in a building with such large floor areas.

Figure 6-30 shows how FDS represented the eight modeled floors (92 through 99) of the undamaged WTC 1. A similar rendition was prepared for floors 78 through 83 of WTC 2. The layout of each floor was developed from architectural drawings and from the information described in Section 5.8. There was a wide range of confidence in the accuracy of these floor plans, varying from high (for the floors occupied by Marsh & McLennan in WTC 1, for which recent and detailed plans were obtained) to low (for most of the space in WTC 2 occupied by Fuji Bank, for which floor plans were not available).

The effects of the aircraft impact were derived from the simulations described in Section 6.8. The portions of walls and floors that were "broken" in those simulations were simply removed from the FDS models of the towers. The furnishings outside the aircraft-damaged regions were assumed to be unmoved and undamaged. The treatment of furnishings within the impact zone is discussed later in this section.

Chapter 6

FDS represented the spaces in which the fires and their effluent were to be modeled as a grid of rectangular cells. These grids included the walls, floors, ceilings, and any other obstructions to the movement of air and fire. In the final simulations, the grid size was 0.5 m x 0.5 m x 0.4 m high (1.6 ft x 1.6 ft x 1.3 ft.). Each floor contained about 125,000 grid cells, and the nature of each cell was updated every 10 ms (100 times every second). The computations were performed using parallel processing, in which the fires on each floor were simulated on a different computer. At the end of each 10 ms update, the processors exchanged information and proceeded to the computations for the next time interval. Each simulation of 105 min of fires for WTC 1 took about a week on eight Xeon computers with a combined 16 GB of memory. The simulations for WTC 2, with fewer floors and 60 min of real time fires, took about half the time.

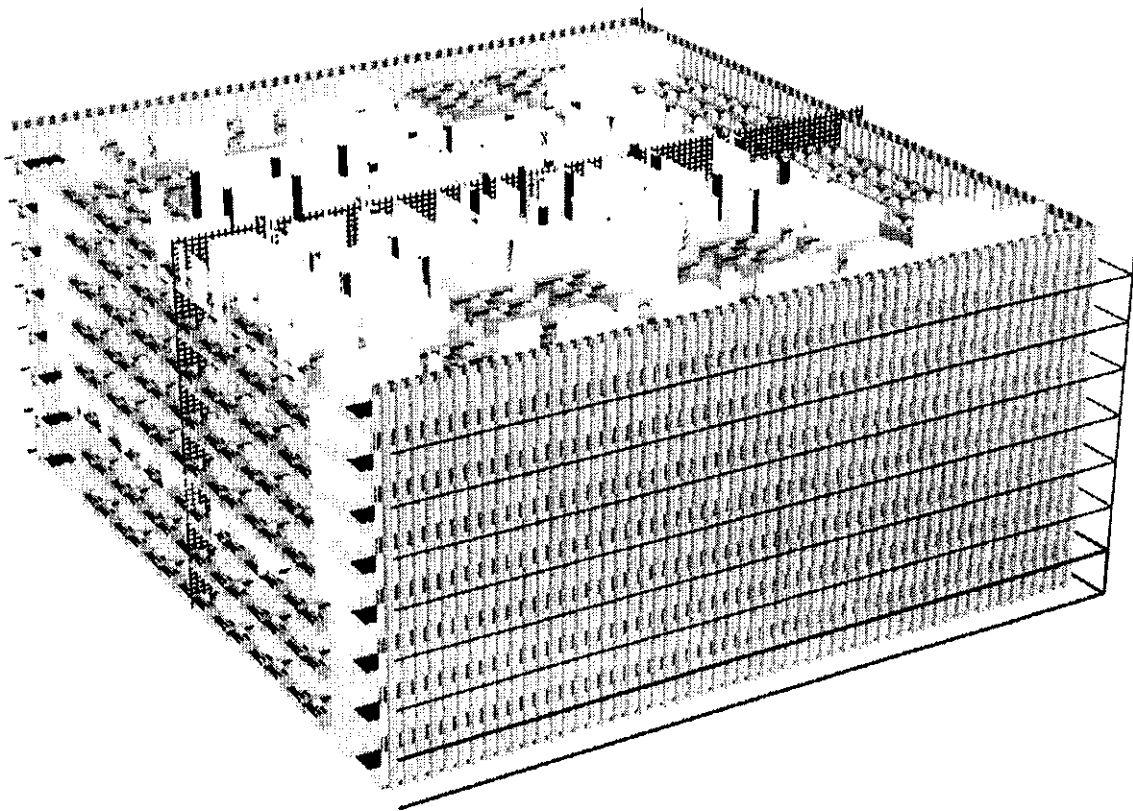
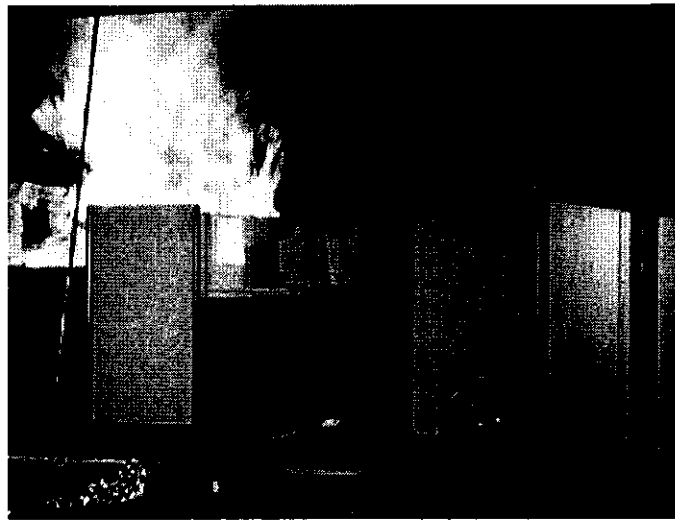


Figure 6–30. Eight floor model of WTC 1 prior to aircraft impact.

The fires were started by ignition of the jet fuel, whose distribution was provided by the aircraft impact simulations. The radiant energy from these short-lived fires heated the nearby combustibles, creating flammable vapors. When these mixed with air in the right proportion within a grid cell, FDS burned the mixture. This generated more energy, which heated the combustibles further, and continued the burning.

The floors of the tower on which the dominant burning occurred were characterized by large clusters of office workstations (Figure 1–11). NIST determined their combustion behavior from a series of single-workstation fire tests (Figure 6–31). In these highly instrumented tests, the effects of workstation type, the presence of jet fuel, and the presence of fallen inert material (such as pieces of ceiling tiles or gypsum board walls) on the burning surfaces were all assessed. While FDS properly captured the gross behavior of these fires, the state of modeling the combustion of real furnishings was still primitive. Thus, the results of this test series were used to refine the combustion module in FDS.



Source: NIST.

Figure 6–31. Fire test of a single workstation.

The accuracy of FDS predictions was then assessed using two different types of fire tests. In each case, the model predictions were generated prior to conducting the test.

The first series provided a measure of the ability of FDS to predict the thermal environment generated by a steady state fire. A spray burner generating 1.9 MW or 3.4 MW of power was ignited in a 23 ft by 11.8 ft by 12.5 ft high compartment. The temperatures near the ceiling approached 900 °C. FDS predicted:

The large fires discussed in this report are characterized by heat release rate, or burning intensity, (in MW), by total energy released (in GJ), and by the heat flux, or radiant intensity (in kW/m²).

- Room temperature increases near the ceiling to within 4 percent.
- Gas velocities at the air inlet to the compartment (and thus the air drawn into the compartment by the fire) within the uncertainty in the experimental measurements.
- The leaning of the fire plume due to the asymmetry of the objects within the compartment. The extent of the leaning was underestimated.
- Radiant heat flux near the ceiling to within 10 percent, within the uncertainty of the experimental measurements.

The second series was a preamble to the modeling of the actual WTC fires. Arrays of three WTC workstations were burned in a 35.5 ft by 23 ft by 11 ft high compartment (Figure 6–32). The tests examined the effects of the type of workstation, the presence of jet fuel, and the presence of fallen inert material on the burning surfaces. In one of the tests, the workstations were rubblized (Figure 6–33). Figure 6–34 depicts the intensity of the test fires. Figure 6–35 shows the measured and predicted heat release rate data from one of the tests in which there was no jet fuel nor inert material present.

Chapter 6



Figure 6–32. Interior view of a three-workstation fire test.

Source: NIST.

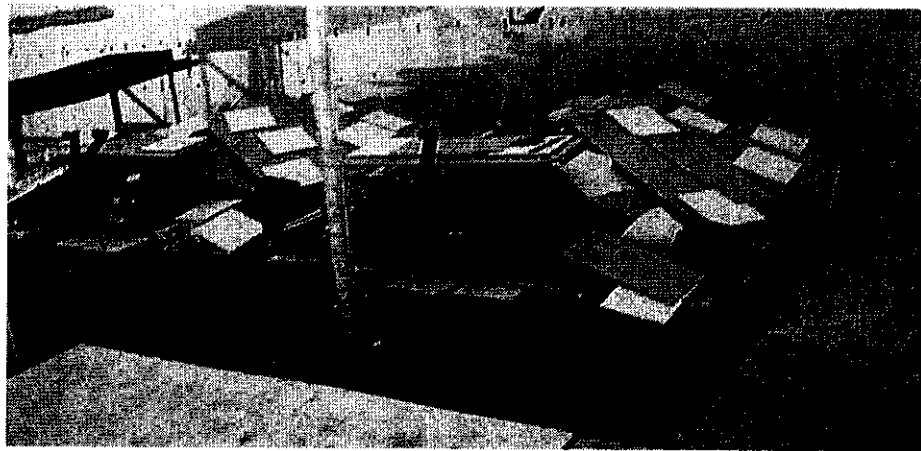


Figure 6–33. Rubblized workstations.

Source: NIST.